Displacement-noise-free gravitational-wave detection with a single Fabry-Perot cavity

Sergey P. Tarabrin and Sergey P. Vyatchanin
*Faculty of Physics, Moscow State University, Moscow, 119992, Russia**
(Dated: September 28, 2007)

We propose a detuned Fabry-Perot cavity, pumped through both the mirrors, as a simple topology of the gravitational-wave (GW) detector free from displacement noise of the test masses. The isolation of the GW signal from displacement noise is achieved in the proper linear combination of the cavity output signals. The construction of such a linear combination is possible due to (i) the equivalence principle and (ii) the asymmetry between reflection and transmission output ports of the detuned cavity. We demonstrate that in low-frequency region the obtained displacement-noise-free response signal is much stronger than the $f_{\rm gw}^3$-limited sensitivity of displacement-noise-free interferometers recently proposed by Y. Chen *et al.* This feature allows to consider the proposed topology a promising prototype of the future-generation GW detector.

PACS numbers: 04.30.Nk, 04.80.Nn, 07.60.Ly, 95.55.Ym

I. INTRODUCTION

Currently the search for gravitational radiation from astrophysical sources is conducted with the first-generation Earth-based laser interferometers [1, 2] (LIGO in USA [3–5], VIRGO in Italy [6, 7], GEO-600 in Germany [8, 9], TAMA-300 in Japan [10, 11] and ACIGA in Australia [12, 13]). The development of the second-generation GW detectors (Advanced LIGO in USA [14, 15], LCGT in Japan [16]) is underway.

The sensitivity of the first-generation detectors is limited by a great amount of noises of various nature: seismic and gravity-gradient noise at low frequencies (below ~ 50 Hz), thermal noise in suspensions, bulks and coatings of the mirrors ($\sim 50 \div 500$ Hz), photon shot noise (above ~ 500 Hz), etc. It is expected that the sensitivity of the second-generation detectors will be limited by the noise of quantum nature arising due to Heisenberg's uncertainty principle: the more precise is the measurement of the test mass coordinate, the more disturbed becomes its momentum which in turn evolves into the disturbance of the coordinate, thus ultimately limiting the sensitivity [17]. The optimum between measurement noise (photon shot noise in laser interferometry) and back-action noise (optical radiation pressure noise) is called the Standard Quantum Limit (SQL) [18–20].

Though the start of operation of the second-generation detectors is planned for the next decade, the theoretical investigations of the third-generation prototypes have already begun [21–26]. It is expected that the barrier of SQL will be overcome and the sensitivity of the third-stage detectors will be two or three orders of magnitude better than the SQL of a free mass.

Recently in a series of papers [27–29] Y. Chen *et al.* proposed several topologies of the GW detectors, both ground- and space-based, which are free from both the displacement noise of the test masses and classical laser noise. It was pointed out there that the latter, in principle, is indistinguishable from the former and therefore, detectors free from both kind of noises were called the displacement-noise-free interferometers (DFI). The most intriguing feature of displacement-noise-free interferometry is the straightforward overcoming of the SQL (since radiation pressure noise is canceled) without the need of implementation of very complicated and vulnerable schemes for Quantum-Non-Demolition (QND) measurements [21, 30–32]. One only needs to increase the laser power to suppress quantum shot noise and achieve the arbitrarily high sensitivity.

Cancelation of laser noise in interferometric experiments is usually achieved by implementing the differential schemes of measurements: in conventional interferometers (such as LIGO) it is the Michelson topology and in DFIs proposed in Ref. [29] it is the Mach-Zehnder (MZ) topology.

The isolation of the GW signal from fluctuating displacements of the test masses in the DFI schemes proposed by Y. Chen *et al.* is possible due to the fact that the interaction of GWs with a laser interferometer is distributed, as viewed from both the transverse-traceless (TT) gauge [33–35] and the local Lorentz (LL) gauge [34, 36, 37].

In the TT gauge test masses are immovable, i.e. have fixed spacial coordinates and thus do not sense the gravitational wave. However, GW couples to the light wave in this gauge producing a non-vanishing phase shift. This can be thought of as an apparent change of the coordinate speed of light. Even if the test masses are not ideally inertial and follow non-geodesic motion then the interferometer will respond differently to the test masses motions and the gravitational wave. This difference allows the cancelation of displacement noise in a proper linear combination of the interferometer response signals.

From the point of view of the local observer (the LL gauge) the interaction of GW with laser interferometer adds up to two effects. The first one is the motion of the test masses in the GW-induced (tidal) force-field. In this aspect GWs are indistinguishable from any external

*Electronic address: tarabrin@phys.msu.ru

non-GW forces since both are sensed by the light wave only in the moments of reflection from the test masses. If the linear scale L of a GW detector is much smaller than the gravitational wavelength $\lambda_{\rm gw}$ (the so-called long-wave approximation) then the effect of GW-induced force-field is of the order of $h(L/\lambda_{\rm gw})^0$, where h is the absolute value of the GW amplitude. Also terms of the order of $O[h(L/\lambda_{\rm gw})^1]$, describing time delays, arise in laser interferometry since it takes the light wave time L/c to travel between the test masses. Second, GW directly couples to the light wave effectively changing the coordinate velocity of light (but in a different manner compared to the TT gauge). In long-wave approximation this effect has the order of $O[h(L/\lambda_{\rm gw})^2]$. Therefore, in terms of the LL gauge the displacement-noise-free interferometry necessarily implies the cancelation of the information about non-GW forces along with the GW-induced tidal force-field leaving a non-vanishing information about the direct coupling of the GW to light.

The analysis performed by Y. Chen *et al.* in Ref. [29] showed, however, that though it is possible to eliminate all the information about the displacement and laser noises from the DFI response signal, the sensitivity to GWs at low frequencies turns out to be limited by the $(\omega_{\rm gw}L/c)^2$-factor for 3D (space-based) configurations and $(\omega_{\rm gw}L/c)^3$-factor for 2D (ground-based) configurations. In the latter case this means the cancelation of all the terms of the order of $h(L/\lambda_{\rm gw})^n$, $n = 0, 1, 2$. For the signals around $\omega_{\rm gw}/2\pi \approx 100$ Hz and $L \approx 4$ km, the DFI sensitivity of the ground-based detector is $\sim 10^6$ times worse than the one of the conventional Michelson interferometer (i.e. a single round-trip detector). The proposed MZ-based configurations could be modified with power- and signal-recycling mirrors [38], artificial time-delay devices [39, 40], but nevertheless, the potentially achievable sensitivity is still incomparable with conventional non-DFI detectors.

In this paper we propose a single detuned Fabry-Perot (FP) cavity operating as the GW detector free from displacement noise of the test masses. If a FP cavity is pumped through both of its mirrors then one can use all the four output ports (reflection and transmission ports for each of the pumps) to properly combine their signals and cancel the fluctuations of test masses positions. Pump waves in different input ports are assumed to be orthogonally polarized in order the corresponding output waves to be separately detectable and to exclude nonlinear coupling of the corresponding intracavity waves. Below we call the proposed scheme a double-pumped Fabry-Perot (DPFP) cavity. In this paper we do not consider the cancelation of laser noise and therefore, the term "displacement noise" will be used below to denote only the displacement noise of the test masses. We will consider a FP cavity with the mirrors having equal transmittances. The case of different transmittances will be analyzed separately [41].

The isolation of the GW signal from displacement noise in the DPFP cavity is achieved in a different manner compared to MZ-based interferometers. The key role is played by two factors. The first one is the (weak) equivalence principle which, in terms of the LL gauge, allows to construct a locally inertial reference frame for a test mass. This in turn allows to separate the deposits of displacement noise and GW signal into the output signals of the DPFP cavity. In terms of the TT gauge this separation is the direct consequence of the distributed nature of GWs. Second, the cancelation of displacement fluctuations in a linear combination of the reflected and transmitted output signals of the *detuned* DPFP cavity implies that these signals differ in the amount of information they carry about the GW signal and the fluctuating displacements. In the resonant regime both the reflected and transmitted signals (corresponding to one of the pumps) carry identical information and thus cannot be combined to cancel fluctuations.

Note that the direct coupling of the GW to light in the LL gauge plays no role in this noise-cancelation scheme: the notion of the GW in our analysis can be reduced to the corresponding tidal force-field. This means that the leading order of the DFI response signal in our case will be $h(L/\lambda_{\rm gw})^0$. From the point of view of the TT gauge this means that the difference between the localized nature of displacement noise and the distributed nature of GWs is utilized in a DPFP cavity in another way compared to the DFIs in Refs. [27–29] (see Sec. IV).

The "payment" for isolation of the GW signal from displacement noise in our case is the loss of the optical resonant gain of the order of $c/(\gamma L)$, where γ is the cavity half-bandwidth. In conventional interferometers this resonant factor describes the accumulation of the low-frequency GW signal by the light wave circulating in a FP cavity. The DFI response signal of the DPFP cavity becomes limited with the factor of the order of unity compared to the limiting factor $(\omega_{\rm gw}L/c)^3 \sim 6 \times 10^{-7}$ of the double Mach-Zehnder configuration [29] for $L \approx 4$ km and $\omega_{\rm gw}/2\pi \approx 100$ Hz. This difference between the MZ-based topologies and the DPFP topology arises due to the different mechanisms of noise cancelation: the former utilizes the effect of the direct coupling of the GW to light in terms of the LL gauge (and thus relies on the cancelation of the $h(L/\lambda_{\rm gw})^0$-term) while the latter utilizes the asymmetry between the output signals of the detuned DPFP cavity (and thus does not rely on the cancelation of the $h(L/\lambda_{\rm gw})^0$-term).

Note that the non-resonant regime implies the rise of the electromagnetic ponderomotive force acting on the mirrors of a FP cavity. This in turn may indicate that the DFI response signal can be further amplified using the optical rigidity-induced optomechanical resonance [42–50]. However, the detailed analysis of radiation pressure effects in a DPFP cavity is the subject of separate consideration [51]; in this paper we do not take into account optical rigidity. In particular, optical rigidity vanishes if pump waves in different input ports have detunings with equal absolute values but opposite signs.

This paper is organized as follows. In Sec. II we de-

rive the response signals of a Fabry-Perot cavity, pumped through one of the mirrors, to a gravitational wave of arbitrary frequency using the method developed in Ref. [37]. In Sec. III we consider a double-pumped Fabry-Perot cavity and obtain the formulas for the signals in all of its output ports. Next we introduce the proper linear combination of the obtained signals which cancels the fluctuating displacements of the test masses. Finally in Sec. IV we discuss the physical meaning of the obtained results, compare DPFP cavity with conventional interferometers and the interferometers proposed by Y. Chen *et al.* and briefly outline the further prospects associated with laser noise cancelation and implementation of the optical rigidity.

II. RESPONSE OF A FABRY-PEROT CAVITY TO A PLANE GRAVITATIONAL WAVE

A. Space-time of the weak plane '+'-polarized gravitational wave

First we introduce the space-time associated with the incident gravitational wave. We assume the latter to be weak, plane and '+'-polarized. In the local Lorentz reference frame of some physical body space-time metric takes the following form [34, 36, 37]:

$$\begin{aligned} ds^2 =& -c^2dt^2 + dx^2 + dy^2 + dz^2 \\ &+ \frac{1}{2c^2}\left(x^2 - y^2\right)\ddot{h}\,(c\,dt - dz)^2, \end{aligned} \tag{1}$$

where $h = h(t - z/c)$, $|h| \ll 1$ is the GW function. Greek indices run over $0, 1, 2, 3$ or ct, x, y, z; Latin indices run over $1, 2, 3$ or x, y, z.

The local Lorentz frame, also called the LL gauge in literature, is the best suited for analysis of the GW detectors with the test masses undergoing non-geodesic motion, in contrast to the transverse-traceless (TT) gauge [36, 37]. Recently it was strictly proven that the LL gauge is free from the requirement of the distance L between the masses to be much smaller than the gravitational wave $\lambda_{\rm gw}$ [52]. Below we call corresponding approximation $L \ll \lambda_{\rm gw}$ the long-wave approximation.

It is worth noting that the case of generic GW polarization and direction of propagation does not introduce any significant changes (in the context of this work) in our further analysis. Therefore, we restrict ourselves to consideration of '+'-polarized gravitational waves traveling along the z-axis.

B. Quantized electromagnetic wave interacting with the weak plane gravitational wave

Here we briefly remind the formalism of the quantized electromagnetic wave (EMW) propagating in the space-time of weak plane gravitational wave.

In this paper we deal with the EMWs which can be represented as a sum of (i) the "strong" (classical) plane monochromatic wave with amplitude A_0 and frequency ω_0 and (ii) the "weak" wave describing quantum fluctuations of the electromagnetic field. In flat space-time the operator of electric field $A(x,t)$ of such EMWs in Heisenberg representation can be written in the following form (see Appendix A):

$$A(x,t) = \sqrt{\frac{2\pi\hbar\omega_0}{Sc}}\,\Big[A_0 + a(x,t)\Big]e^{-i(\omega_0 t \mp k_0 x)} + \text{h.c.}, \tag{2a}$$

$$a(x,t) = \int_{-\infty}^{+\infty} a(\omega_0 + \Omega)e^{-i\Omega(t \mp x/c)}\,\frac{d\Omega}{2\pi}, \tag{2b}$$

with amplitude $a(\omega_0 + \Omega)$ obeying the commutation relations:

$$\begin{aligned} &\big[a(\omega_0 + \Omega), a(\omega_0 + \Omega')\big] = 0, \\ &\big[a(\omega_0 + \Omega), a^\dagger(\omega_0 + \Omega')\big] = 2\pi\delta(\Omega - \Omega'). \end{aligned}$$

This notation for quantum fluctuations $a(x,t)$ will be the most suitable for us since it coincides exactly with the Fourier-representation of the classical fields. If the phase is counted from $x = x_0 \neq 0$ then one should replace in formulas (2a, 2b) $e^{\pm ik_0 x} \to e^{\pm ik(x - x_0)}$ and $e^{\pm i\Omega x/c} \to e^{\pm i\Omega(x - x_0)/c}$. For briefness throughout the paper we omit the $\sqrt{2\pi\hbar\omega_0/Sc}$-multiplier and notation "h.c." We call $A(x,t)$ the vacuum-state wave if $A_0 = 0$.

If space-time is curved then electromagnetic field is coupled to gravitational field. In our case we assume that the weak GW is coupled only to the "strong" electromagnetic wave and neglect its interaction with (i) the optical noise and (ii) the variation of EMW due to GW itself. In other words we consider the first-order-of-h theory. Electromagnetic wave propagating on the background metric (1) is described by the following formula [37]:

$$A(x,t) = \Big[A_0 + A_0 g_\pm(x,t) + a(x,t)\Big]e^{-i(\omega_0 t \mp k_0 x)}, \tag{3a}$$

$$g_\pm(x,t) = \int_{-\infty}^{+\infty} g_\pm(x, \omega_0 + \Omega)e^{-i\Omega t}\,\frac{d\Omega}{2\pi}, \tag{3b}$$

$$\begin{aligned} g_\pm(x, \omega_0 + \Omega) = h(\Omega)\bigg[&\frac{1}{4}\,\omega_0\Omega\,\frac{x^2}{c^2} \mp i\,\frac{1}{2}\,k_0 x \\ &+ \frac{1}{2}\,\frac{\omega_0}{\Omega}\,\Big(e^{\pm i\Omega x/c} - 1\Big)\bigg], \end{aligned} \tag{3c}$$

where $g_\pm(x,t)$ are accurate up to the order of $(\Omega/\omega_0)^0$. Terms containing $g_\pm$ describe the direct coupling of the GW to the EMW. Remind [37], that in the long-wave approximation $g_\pm = O[h(L/\lambda_{\rm gw})^2]$. It is also straightforward to verify using formulas (3b, 3c) that $g_\pm(x,t)$ are the pure imaginary values. Therefore, sometimes it will be convenient to use the following approximate formula:

$$1 + g_\pm(x,t) = 1 + i\Im\big[g_\pm(x,t)\big] \approx e^{i\Im\left[g_\pm(x,t)\right]}. \tag{4}$$

Below we assume all the waves to be described by formulas (3a – 3c) with corresponding indices and initial phases.

C. Input, circulating and output waves

Let us consider now a Fabry-Perot cavity formed by two movable mirrors a and b (see Fig. 1), both lossless and having the amplitude transmission coefficient T, $|T| \ll 1$. We put distance between the mirrors in the absence of the gravitational wave and optical radiation to be equal to L. Without the loss of generality we assume the cavity to be lying in the plane $z = 0$ along one of the GW principal axes, coinciding with the x-axis.

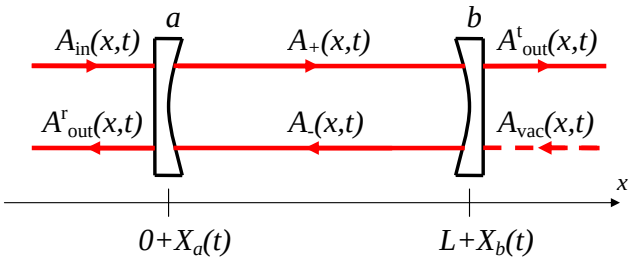

FIG. 1: Fabry-Perot cavity formed by two movable mirrors a and b. Their coordinates are $x_a(t) = 0 + X_a(t)$ and $x_b(t) = L + X_b(t)$ respectively with $|X_{a,b}| \ll L$. Both the mirrors have amplitude transmission coefficient T with $|T| \ll 1$. Cavity is pumped through mirror a with the input wave $A_{\rm in}(x,t)$ and through mirror b with the vacuum-state wave $A_{\rm vac}(x,t)$. Optical field inside the cavity is represented as a sum of the wave $A_+(x,t)$, running in the positive direction of the x-axis, and the wave $A_-(x,t)$, running in the opposite direction. The reflection-output signal is $A^{\rm r}_{\rm out}(x,t)$ and transmission-output signal is $A^{\rm t}_{\rm out}(x,t)$.

In this section we will work in the local Lorentz reference frame of mirror a at which the origin of the coordinate system is set. Then the coordinates (their operators to be strict) of the mirrors are $x_a(t) = 0 + X_a(t)$ and $x_b(t) = L + X_b(t)$ and we assume that their displacements $X_{a,b}(t)$ from the positions of equilibrium obey the relation $|X_{a,b}| \ll L$. In spectral domain

$$X_{a,b}(t) = \int_{-\infty}^{+\infty} X_{a,b}(\Omega) e^{-i\Omega t}\, \frac{d\Omega}{2\pi}.$$

Let the cavity be pumped by laser L through mirror a (see Fig. 2) with the input wave

$$\begin{aligned} A_{\rm in}(x,t) =& A_{\rm in0}\big[1 + g_+(x,t)\big] e^{-i(\omega_1 t - k_1 x)} \\ &+ a_{\rm in}(x,t) e^{-i(\omega_1 t - k_1 x)}, \end{aligned} \tag{5}$$

and with the vacuum-state wave through mirror b:

$$A_{\rm vac}(x,t) = a_{\rm vac}(x,t) e^{-i\left[\omega_1 t + k_1 (x-L)\right]}, \tag{6}$$

Here $a_{\rm in}(x,t)$ is the "weak" field describing laser noise of the pump wave and $a_{\rm vac}(x,t)$ is the "weak" field describing vacuum noise in another input port. We count phases of the input wave and the vacuum-state wave from $x = 0$ and $x = L$ correspondingly.

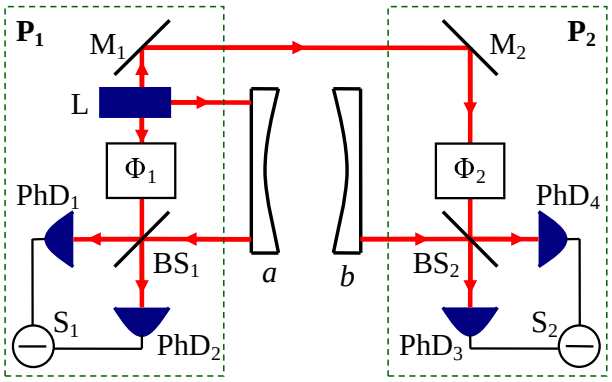

FIG. 2: Emission-detection scheme. Pump wave is radiated by laser L. Reflected wave is measured with the left homodyne detector assembled of homodyne phase shifter Φ_1, 50/50-beamsplitter $\rm BS_1$, two photodetectors $\rm PhD_{1,2}$ and subtractor $\rm S_1$. Transmitted wave is measured with the right homodyne detector assembled of homodyne phase shifter Φ_2, 50/50-beamsplitter $\rm BS_2$, two photodetectors $\rm PhD_{3,4}$ and subtractor $\rm S_2$. Laser L, mirror $\rm M_1$ and left homodyne detector are assumed to be rigidly installed on the platform $\rm P_1$ and right homodyne detector with mirror $\rm M_2$ are rigidly installed on the platform $\rm P_2$. The coordinate of platform $\rm P_1$ is $x_{\rm P_1}(t) = 0 - l_{\rm P_1} + X_{\rm P_1}(t)$ with $l_{\rm P_1}, X_{\rm P_1} \ll L$, where $l_{\rm P_1}$ is the distance between mirror a and platform $\rm P_1$ in the state of rest and $X_{\rm P_1}(t)$ is the displacement of platform $\rm P_1$ from the position of equilibrium. Similarly, the coordinate of platform $\rm P_2$ is $x_{\rm P_2}(t) = L + l_{\rm P_2} + X_{\rm P_2}(t)$ with $l_{\rm P_2}, X_{\rm P_2} \ll L$, where $l_{\rm P_2}$ is the distance between mirror b and platform $\rm P_2$ in the state of rest and $X_{\rm P_2}(t)$ is the displacement from the position of equilibrium.

It is convenient to represent the optical field inside the cavity as a sum of two waves, $A_+(x,t)$ and $A_-(x,t)$, running in the opposite directions:

$$\begin{aligned} A_\pm(x,t) =& A_{\pm 0}\big[1 + g_\pm(x,t)\big] e^{-i(\omega_1 t \mp k_1 x)} \\ &+ a_\pm(x,t) e^{-i(\omega_1 t \mp k_1 x)}. \end{aligned} \tag{7}$$

Phases of both the waves are counted from $x = 0$. Here $a_\pm(x,t)$ describes the phase shift accumulated by the light wave while circulating inside the cavity.

Output wave reflected from the cavity is:

$$\begin{aligned} A^{\rm r}_{\rm out}(x,t) =& A^{\rm r}_{\rm out0}\big[1 + g_-(x,t)\big] e^{-i(\omega_1 t + k_1 x)} \\ &+ a^{\rm r}_{\rm out}(x,t) e^{-i(\omega_1 t + k_1 x)}, \end{aligned} \tag{8}$$

with its phase counted from $x = 0$. Quadrature components (see Appendix A) of the reflected wave (of $a^{\rm r}_{\rm out}(x,t)$ to be strict — see below) are assumed to be measured with the left homodyne detector located on platform $\rm P_1$ (see Fig. 2) assembled of homodyne phase shifter Φ_1, beamsplitter $\rm BS_1$, two photodetectors $\rm PhD_{1,2}$ and subtractor $\rm S_1$. The reference oscillation is produced by laser L.

Output wave transmitted through the cavity is:

$$A^{\rm t}_{\rm out}(x,t) = A^{\rm t}_{\rm out0}\big[1+g_+(x,t)\big]e^{-i\left[\omega_1 t - k_1(x-L)\right]} + a^{\rm t}_{\rm out}(x,t)e^{-i\left[\omega_1 t - k_1(x-L)\right]}. \quad (9)$$

with its phase counted from $x = L$. Quadratures of the transmitted wave (of $a^{\rm t}_{\rm out}(x,t)$ to be strict — see below) are measured with the right homodyne detector assembled of homodyne phase shifter Φ_2, beamsplitter $\rm BS_2$, two photodetectors $\rm PhD_{3,4}$ and subtractor $\rm S_2$. The reference oscillation is produced by laser L. We do not consider the situation when reference oscillation is produced by the additional laser synchronized with laser L and located on the platform $\rm P_2$.

Below we assume that laser L, mirror $\rm M_1$ and left homodyne detector are rigidly installed on a single platform $\rm P_1$, i.e. all the elements on platform $\rm P_1$ do not move with respect to each other. In addition, we assume all the distances between mirror a and all the elements on platform $\rm P_1$ to be much smaller than the length of the cavity L. We characterize all these distances with a single parameter $l_{\rm P_1}$. This assumption means that in the field of a GW the local Lorentz reference frame of mirror a and the one of platform $\rm P_1$ approximately coincide and therefore, according to formula (14a) (see below), platform $\rm P_1$ undergoes fluctuating motion only. The similar considerations hold true for the mirror b and platform $\rm P_2$ with $l_{\rm P_2} \ll L$ being the mean distance between the mirror and the platform. Thus in the local Lorentz frame of mirror a the second mirror and platform $\rm P_2$ undergo GW displacement $\frac{1}{2}Lh(t)$ along with their fluctuating displacements (see formula (14b) below).

The measurement scheme in Fig. 2 does not allow to detect the additional GW-induced phase shift described by the first term in formula (9) which corresponds to the propagation of the optical-noiseless light wave in the GW field in the absence of the cavity (i.e. in the limit $R \to 0$). At point $x = x_{\rm P_2}(t) \approx L + \frac{1}{2}Lh(t)$ the first summand in formula (9) approximately equals to (neglecting the fluctuations)

$$A^{\rm t}_{\rm out0}\big[1+g_+(x_{P_2},t)\big]e^{-i\left[\omega_1 t - k_1(x_{\rm P_2}-L)\right]} \approx A^{\rm t}_{\rm out0}\exp\left\{i\frac{1}{2}\,k_1 Lh(t) + i\Im\big[g_+(L,t)\big]\right\}e^{-i\omega_1 t}.$$

Here we used formula (4) to write down the single-pass GW-induced phase shift $\frac{1}{2}\,k_1 Lh(t) + \Im\big[g_+(L,t)\big]$ explicitly. However, the same GW-induced phase shift is also presented in the phase of the reference oscillation — the light wave produced by laser L traveling from mirror $\rm M_1$ through $\rm M_2$ to the right homodyne detector (see Fig. 2). Ultimately, both the phases of the transmitted wave and of the reference oscillation are completely subtracted in the homodyne measurement (see details in Appendix B).

Obviously, in order the first term in formula (9) to be measurable, one should change the detection scheme on platform $\rm P_2$ in such a way that the local oscillator (additional laser perfectly synchronized with laser L on platform $\rm P_1$) for the transmitted wave would be placed on platform $\rm P_2$. In this case the reference oscillation does not acquire the additional GW-induced phase and therefore, the first term in formula (9) does not vanish in the balanced homodyne detection. Remind, that in this paper we do not consider the configuration of detection scheme for a single-pumped FP cavity with the local oscillator placed on platform P_2

Therefore, the measurable quantities in our case are the quadrature components of $a^{\rm r}_{\rm out}$ and $a^{\rm t}_{\rm out}$. Complex amplitudes (operators to be strict) $a^{\rm r}_{\rm out}(x,t)$ and $a^{\rm t}_{\rm out}(x,t)$ are the unknown functions of their arguments which are obtained as the solutions of the corresponding boundary problem for a FP cavity (see below). Obviously, they should vanish in the limit $R \to 0$ (see formulas (11a, 11b) below), i.e. in the absence of the cavity, if $a_{\rm in} = a_{\rm vac} \equiv 0$. Therefore, below we call functions $a^{\rm r,t}_{\rm out}(x,t)$ or $a^{\rm r,t}_{\rm out}(\omega_1+\Omega)$ the cavity response (or output) signals, meaning that they describe the influence of a FP cavity on the light propagation. The first terms in formulas (8) and (9) thus correspond to the "no-cavity" case and are not interested for us: our detection scheme is constructed in such a way that these terms become unmeasurable.

Note that we do not require the platforms $\rm P_{1,2}$ to be ideally inertial bodies: the information about displacement noise of platform $\rm P_1$ is equivalent to laser noise which can be further canceled and displacement noise of platform $\rm P_2$ is eliminated by the balanced homodyne detection schemes in full similarity with the cancelation of the (single-pass) GW-induced phase shift as discussed above (see Appendix B).

D. Response signals of a Fabry-Perot cavity

To obtain the response functions of a Fabry-Perot cavity we substitute fields (5 – 9) into the set of boundary conditions (conditions of the electric field continuity along the surfaces of the mirrors) [37, 53]:

$$A_+(x_a,t) = TA_{\rm in}(x_a,t) - RA_-(x_a,t), \quad (10a)$$
$$A^{\rm r}_{\rm out}(x_a,t) = RA_{\rm in}(x_a,t) + TA_-(x_a,t), \quad (10b)$$
$$A_-(x_b,t) = TA_{\rm vac}(x_b,t) - RA_+(x_b,t), \quad (10c)$$
$$A^{\rm t}_{\rm out}(x_b,t) = RA_{\rm vac}(x_b,t) + TA_+(x_b,t). \quad (10d)$$

This set of equations is accurate up to the zeroth order of Ω/ω_1 since it does not take into account the relativistic terms proportional to $\dot{X}_{a,b}/c$ [37]. The solution of this set is obtained in Appendix C using the method of successive approximations. Since we do not consider the effect of parametric excitation of the additional optical modes under the influence of the GW [37], it will be convenient to introduce the detuning $\delta_1 = \omega_1 - \pi n_0/\tau$, where n_0 is integer, even (for simplicity) and fixed. Then the solution of the first order takes the following form (all spectral arguments are omitted):

$$a^{\rm r}_{\rm out} = \frac{R - Re^{2i(\delta_1+\Omega)\tau}}{1 - R^2 e^{2i(\delta_1+\Omega)\tau}}\, a_{\rm in} + \frac{T^2 e^{i(\delta_1+\Omega)\tau}}{1 - R^2 e^{2i(\delta_1+\Omega)\tau}}\, a_{\rm vac} - \frac{RT^2 A_{\rm in0} e^{2i\delta_1\tau}}{1 - R^2 e^{2i\delta_1\tau}}\, i\, \frac{2k_1(X_b e^{i\Omega\tau} - \sigma X_a) + \delta\Psi_{\rm gw+emw}}{1 - R^2 e^{2i(\delta_1+\Omega)\tau}}, \tag{11a}$$

$$a^{\rm t}_{\rm out} = \frac{T^2 e^{i(\delta_1+\Omega)\tau}}{1 - R^2 e^{2i(\delta_1+\Omega)\tau}}\, a_{\rm in} + \frac{R - Re^{2i(\delta_1+\Omega)\tau}}{1 - R^2 e^{2i(\delta_1+\Omega)\tau}}\, a_{\rm vac} + \frac{R^2 T^2 A_{\rm in0} e^{3i\delta_1\tau}}{1 - R^2 e^{2i\delta_1\tau}}\, i\, \frac{2k_1(X_b e^{i\Omega\tau} - X_a) + \delta\Psi_{\rm gw+emw}}{1 - R^2 e^{2i(\delta_1+\Omega)\tau}}\, e^{i\Omega\tau}. \tag{11b}$$

Here $\tau = L/c$. Phase shift

$$\delta\Psi_{\rm gw+emw}(\Omega) = -ik_1 Lh(\Omega)\left(1 - \frac{\sin\Omega\tau}{\Omega\tau}\right), \tag{12}$$

calculated in the approximation $\Omega/\omega_1 \ll 1$, describes the direct coupling of the gravitational wave to the light wave, and factor

$$\sigma_1(\Omega) = e^{-2i\delta_1\tau}/T^2 \times \Big[1 - R^2 e^{2i\delta_1\tau} - R^2 e^{2i(\delta_1+\Omega)\tau} + R^2 e^{2i(2\delta_1+\Omega)\tau}\Big],$$

describes the difference between $a^{\rm r}_{\rm out}$ and $a^{\rm t}_{\rm out}$ of the detuned cavity, playing the key role in our further consideration. In the resonant regime ($\delta = 0$) we have $\sigma_1 = 1$ and $a^{\rm t}_{\rm out} = Ra^{\rm r}_{\rm out} e^{i\Omega\tau}$ or $a^{\rm t}_{\rm out}(t) = Ra^{\rm r}_{\rm out}(t-\tau)$ in time domain. Thus it is convenient to rewrite factor σ_1 as a sum $1 + \Delta\sigma_1$, where:

$$\Delta\sigma_1 = \left(1 - e^{2i\delta_1\tau}\right)\frac{\mathcal{T}^2_{\delta_1+\Omega}}{T^2}\, e^{-2i\delta_1\tau}, \tag{13}$$

(see notation for $\mathcal{T}^2_{\delta_1+\Omega}$ below) is the measure of the asymmetry between the output signals.

Now we split the displacements $X_{a,b}$ into geodesic and fluctuating. We denote the latter with $\xi_{a,b}$. In the local Lorentz frame of mirror a the latter falls freely in the GW field and

$$X_a(t) = 0 + \xi_a(t), \tag{14a}$$

$$X_b(t) = \frac{1}{2} Lh(t) + \xi_b(t). \tag{14b}$$

These formulas are strict for any separation between the mirrors [36, 37]. Note that the GW function $h(t)$ is included in the law of motion of only the single test mass, not the both. Substituting these formulas into the cavity response signals (11b, 11a) we rewrite them in terms of the GW signal

$$\xi_{\rm gw}(\Omega) = \frac{1}{2} Lh(\Omega)\, \frac{\sin\Omega\tau}{\Omega\tau},$$

and fluctuating displacements $\xi_{a,b}$:

$$a^{\rm r}_{\rm out} = \mathcal{R}_1 a_{\rm in} + \mathcal{T}_1 a_{\rm vac} - \frac{RT^2 A_{\rm in0} e^{2i\delta_1\tau}}{\mathcal{T}^2_{\delta_1}\mathcal{T}^2_{\delta_1+\Omega}}\, 2ik_1\Big[\xi_b e^{i\Omega\tau} - \sigma_1\xi_a + \xi_{\rm gw} e^{i\Omega\tau}\Big], \tag{15a}$$

$$a^{\rm t}_{\rm out} = \mathcal{T}_1 a_{\rm in} + \mathcal{R}_1 a_{\rm vac} + \frac{R^2 T^2 A_{\rm in0} e^{3i\delta_1\tau}}{\mathcal{T}^2_{\delta_1}\mathcal{T}^2_{\delta_1+\Omega}}\, 2ik_1\Big[\xi_b e^{i\Omega\tau} - \xi_a + \xi_{\rm gw} e^{i\Omega\tau}\Big] e^{i\Omega\tau}. \tag{15b}$$

The following notations have been introduced above:

$$\mathcal{T}^2_{\delta_1} = 1 - R^2 e^{2i\delta_1\tau}, \qquad \mathcal{T}^2_{\delta_1+\Omega} = 1 - R^2 e^{2i(\delta_1+\Omega)\tau},$$

$$\mathcal{R}_1 = \frac{R - Re^{2i(\delta_1+\Omega)\tau}}{1 - R^2 e^{2i(\delta_1+\Omega)\tau}}, \qquad \mathcal{T}_1 = \frac{T^2 e^{i(\delta_1+\Omega)\tau}}{1 - R^2 e^{2i(\delta_1+\Omega)\tau}},$$

having the following physical meaning: $1/\mathcal{T}^2_{\delta_1}$ describes the resonant amplification of the input amplitude $A_{\rm in0}$ inside the cavity, $1/\mathcal{T}^2_{\delta_1+\Omega}$ describes the frequency-dependent resonant amplification of the variation $a_\pm$ of the circulating light wave, $\mathcal{R}_1$ and $\mathcal{T}_1$ are the generalized coefficients of reflection (from a FP cavity) and transmission (through a FP cavity).

III. DOUBLE-PUMPED FABRY-PEROT CAVITY

A. Response signals of a double-pumped Fabry-Perot cavity

Let a single Fabry-Perot cavity be pumped through both of its mirrors (see Fig. 3). We assume the pump wave through mirror a to have amplitude $\mathcal{A}$, detuning δ_1 (carrier frequency ω_1), polarization in the plane of incidence and denote it with $A_{\rm in}$; the pump wave through mirror b is assumed to have amplitude $\mathcal{B}$, detuning δ_2 (carrier frequency ω_2), polarization orthogonal to the plane of incidence and is denoted with $B_{\rm in}$. Corresponding vacuum pumps through mirrors b and a are denoted with $A_{\rm vac}$ and $B_{\rm vac}$.

The response functions corresponding to the pump through mirror b are straightforwardly obtained from functions (15a, 15b) replacing $\delta_1 \to \delta_2$, $\xi_a \to -\xi_b$, $\xi_b \to -\xi_a$ and keeping the GW term unchanged due to the symmetry of the problem (plane GW wavefront). For convenience we gather signals in all the four output ports of the DPFP cavity omitting spectral arguments and taking into account the relation $k_1 \approx k_2 \equiv k_0$ valid for the corresponding carrier frequencies ω_1 and ω_2 lying within the same resonance curve:

$$a^{\rm r}_{\rm out} = \mathcal{R}_1 a_{\rm in} + \mathcal{T}_1 a_{\rm vac} - \frac{RT^2 \mathcal{A} e^{2i\delta_1\tau}}{\mathcal{T}^2_{\delta_1}\mathcal{T}^2_{\delta_1+\Omega}}\, 2ik_0\Big[(\xi_b + \xi_{\rm gw})e^{i\Omega\tau} - \sigma_1\xi_a\Big], \tag{16a}$$

FIG. 3: Fabry-Perot cavity pumped through both of its mirrors (a DPFP cavity). The pump wave through mirror a is denoted with $A_{\rm in}$ and is assumed to be polarized in the plane of incidence. The pump wave through mirror b is denoted with $B_{\rm in}$ and is assumed to be polarized normally to the plane of incidence. Corresponding vacuum pumps are $A_{\rm vac}$ and $B_{\rm vac}$. Output ports are $A^{\rm r,t}_{\rm out}$ and $B^{\rm r,t}_{\rm out}$.

$$a^{\rm t}_{\rm out} = \mathcal{T}_1 a_{\rm in} + \mathcal{R}_1 a_{\rm vac} + \frac{R^2T^2\mathcal{A}e^{3i\delta_1\tau}}{\mathcal{T}^2_{\delta_1}\mathcal{T}^2_{\delta_1+\Omega}}\, 2ik_0\Big[(\xi_b+\xi_{\rm gw})e^{2i\Omega\tau} - \xi_a e^{i\Omega\tau}\Big], \quad (16b)$$

$$b^{\rm r}_{\rm out} = \mathcal{R}_2 b_{\rm in} + \mathcal{T}_2 b_{\rm vac} - \frac{RT^2\mathcal{B}e^{2i\delta_2\tau}}{\mathcal{T}^2_{\delta_2}\mathcal{T}^2_{\delta_2+\Omega}}\, 2ik_0\Big[(-\xi_a+\xi_{\rm gw})e^{i\Omega\tau} + \sigma_2\xi_b\Big], \quad (16c)$$

$$b^{\rm t}_{\rm out} = \mathcal{T}_2 b_{\rm in} + \mathcal{R}_2 b_{\rm vac} + \frac{R^2T^2\mathcal{B}e^{3i\delta_2\tau}}{\mathcal{T}^2_{\delta_2}\mathcal{T}^2_{\delta_2+\Omega}}\, 2ik_0\Big[(-\xi_a+\xi_{\rm gw})e^{2i\Omega\tau} + \xi_b e^{i\Omega\tau}\Big]. \quad (16d)$$

Here quantities $\mathcal{R}$, $\mathcal{T}$, $\mathcal{T}^2_\delta$ and $\mathcal{T}^2_{\delta+\Omega}$ with the subscripts "1" and "2" are evaluated for detunings δ_1 and δ_2 correspondingly. Note that in the pair of signals $a^{\rm r,t}_{\rm out}$ the GW term $\xi_{\rm gw}$ enters the expression together with ξ_b, but noth with both the ξ_a and ξ_b. The similar statement can be made about the pair $b^{\rm r,t}_{\rm out}$ with corresponding replacements.

The quadrature components of field amplitudes (16c) and (16d) can be detected in a way similar to the case of a single-pumped FP cavity (corresponding to field amplitudes (16a) and (16b)). The emission-detection scheme of a DPFP cavity will require the second laser to produce the second pump and two more homodyne detectors to measure the output signals corresponding to the second pump. The explicit analysis performed in Appendix B remains valid.

B. Cancelation of displacement noise

1. *Field amplitudes*

For the methodological purposes we will first demonstrate the noise cancelation from the combination of field amplitudes (16a – 16d). Though it is obvious and enough from the theoretical point of view, such a consideration is surely insufficient for the experimental purposes, because we can only detect quadrature components of the fields, not the complex field amplitudes themselves.

Anyway, let us assume that the response signals (16a – 16d) have been somehow measured and stored in the computer memory. In three steps we can exclude the information about the fluctuating displacements $\xi_{a,b}$ from the obtained data.

First, we cancel the information about ξ_a from the first pair of signals $a^{\rm r,t}_{\rm out}$. Multiplying $a^{\rm r}_{\rm out}$ on $Re^{i(\delta_1+\Omega)\tau}$ and adding it to $\sigma_1 a^{\rm t}_{\rm out}$ we obtain:

$$\begin{aligned} s_1 &= Re^{i(\delta_1+\Omega)\tau}a^{\rm r}_{\rm out} + \sigma_1 a^{\rm t}_{\rm out} \\ &= s^{\rm fl}_1 + \frac{R^2T^2\mathcal{A}e^{3i\delta_1\tau}}{\mathcal{T}^2_{\delta_1}\mathcal{T}^2_{\delta_1+\Omega}}\, 2ik_0\Delta\sigma_1(\xi_b+\xi_{\rm gw})e^{2i\Omega\tau} \\ &= s^{\rm fl}_1 + R^2e^{i\delta_1\tau}\big(1-e^{2i\delta_1\tau}\big)\,\frac{\mathcal{A}}{\mathcal{T}^2_{\delta_1}}\, 2ik_0(\xi_b+\xi_{\rm gw})e^{2i\Omega\tau}, \end{aligned} \quad (17)$$

$$s^{\rm fl}_1 = a_{\rm in}e^{-i(\delta_1-\Omega)\tau} + \frac{R}{T^2}\Big[e^{2i\Omega\tau}(e^{2i\delta_1\tau}-1) + \mathcal{T}^2_{\delta_1}e^{-2i\delta_1\tau}\Big]a_{\rm vac}.$$

Second, we cancel the information about $-\xi_a+\xi_{\rm gw}$ from the second pair of signals $b^{\rm r,t}_{\rm out}$. Multiplying $b^{\rm r}_{\rm out}$ on $Re^{i(\delta_2+\Omega)\tau}$ and adding it to $b^{\rm t}_{\rm out}$ we obtain:

$$\begin{aligned} s_2 &= Re^{i(\delta_2+\Omega)\tau}b^{\rm r}_{\rm out} + b^{\rm t}_{\rm out} \\ &= s^{\rm fl}_2 - \frac{R^2T^2\mathcal{B}e^{3i\delta_2\tau}}{\mathcal{T}^2_{\delta_2}\mathcal{T}^2_{\delta_2+\Omega}}\, 2ik_0\Delta\sigma_2\xi_b e^{i\Omega\tau} \\ &= s^{\rm fl}_2 - R^2e^{i\delta_2\tau}\big(1-e^{2i\delta_2\tau}\big)\,\frac{\mathcal{B}}{\mathcal{T}^2_{\delta_2}}\, 2ik_0\xi_b e^{i\Omega\tau}, \end{aligned} \quad (18)$$

$$s^{\rm fl}_2 = b_{\rm in}e^{i(\delta_2+\Omega)\tau} + Rb_{\rm vac}.$$

To perform the last step we need to introduce the relation between $\mathcal{A}$ and $\mathcal{B}$. It is convenient (but not necessary) to assume $\mathcal{A}/\mathcal{T}^2_{\delta_1} = \mathcal{B}/\mathcal{T}^2_{\delta_2}$. Then we cancel the information about ξ_b from the pair of signals $s_{1,2}$:

$$\begin{aligned} s &= s_1 + \frac{e^{i\delta_1\tau}\big(1-e^{2i\delta_1\tau}\big)}{e^{i\delta_2\tau}\big(1-e^{2i\delta_2\tau}\big)}\, s_2e^{i\Omega\tau} \\ &= s^{\rm fl} + \frac{R^2T^2\mathcal{A}e^{3i\delta_1\tau}}{\mathcal{T}^2_{\delta_1}\mathcal{T}^2_{\delta_1+\Omega}}\, 2ik_0\Delta\sigma_1\xi_{\rm gw}e^{2i\Omega\tau} \\ &= s^{\rm fl} + R^2e^{i\delta_1\tau}\big(1-e^{2i\delta_1\tau}\big)\frac{\mathcal{A}}{\mathcal{T}^2_{\delta_1}}\, 2ik_0\xi_{\rm gw}e^{2i\Omega\tau}, \end{aligned} \quad (19)$$

$$s^{\rm fl} = a_{\rm in}e^{-i(\delta_1-\Omega)\tau} + \frac{1-e^{2i\delta_1\tau}}{1-e^{2i\delta_2\tau}}\, b_{\rm in}e^{i(\delta_1+2\Omega)\tau} + \frac{R}{T^2}\Big[e^{2i\Omega\tau}\big(e^{2i\delta_1\tau}-1\big) + \mathcal{T}^2_{\delta_1}e^{-2i\delta_1\tau}\Big]a_{\rm vac} + \frac{e^{i\delta_1\tau}\big(1-e^{2i\delta_1\tau}\big)}{e^{i\delta_2\tau}\big(1-e^{2i\delta_2\tau}\big)}\, Rb_{\rm vac}e^{i\Omega\tau}.$$

The total signal s does not contain any information about displacement noise of the test masses and will be called below the DFI response signal.

For the ground-based detectors with the spacial scale L of several kilometers the most important is the low-frequency response, i.e. the limit $\Omega L/c \ll 1$. We will analyze two special cases.

In the simplest case of equal pumps we have $\mathcal{A} = \mathcal{B}$ and $\delta_1 = \delta_2$. Then in the narrow-band approximation ($T^2 = 2\gamma\tau \ll 1$, $\delta_{1,2}\tau \ll 1$, where γ is the cavity half-bandwidth):

$$s|_{\delta_2=\delta_1} \approx a_{\rm in} + b_{\rm in} + a_{\rm vac} + b_{\rm vac} - \frac{i\delta_1}{\gamma - i\delta_1}\,\mathcal{A}\,2ik_0Lh. \quad (20)$$

Remind [42–46], that due to the significant amplification of the input laser power inside the FP cavity test masses are subjected to the force of radiation pressure. It is known that the sign of the induced ponderomotive rigidity depends on the signs of detunings δ_1 and δ_2. Therefore, in order to cancel the effects of radiation pressure we should consider the pumps with opposite detunings $\delta_2 = -\delta_1$. In this case both the pumps create ponderomotive rigidities with opposite signs and the total rigidity vanishes. The DFI signal in this case is:

$$s|_{\delta_2=-\delta_1} \approx a_{\rm in} - b_{\rm in} + a_{\rm vac} - b_{\rm vac} - \frac{i\delta_1}{\gamma - i\delta_1}\,\mathcal{A}\,2ik_0Lh. \quad (21)$$

Obviously, in the previous case of equal detunings total ponderomotive rigidity does not vanish and, strictly speaking, the effects of radiation pressure in the DPFP cavity require detailed analysis [51]. One may expect further amplification of the DFI response signal due to the optomechanical resonance (see Sec. IV).

From the formulas (20) and (21) we conclude that the signal-to-noise ratio of the DPFP cavity operating as the displacement-noise-free detector is of the same order as for the configuration with two test masses and only one round trip of light between them (i.e. without the resonant gain).

2. *Quadratures*

In a real experiment we can only detect the quadrature components of the fields. Once detected, they can be stored in the computer memory for later processing. Therefore, we propose the following scheme of the displacement-noise-free measurement: first, we detect and memorize the quadratures (cosine or sine) of the four output signals; second, we manually, i.e. with a computer, construct the proper linear combination of the quadratures which does not contain the displacement noise.

Here we consider the case of the cosine quadratures being measured (see Appendix B for the details of measurement scheme). We denote the Fourier image of the cosine quadrature corresponding to the optical field amplitude $a(\omega_0 + \Omega)$ as $\mathfrak{a}(\Omega)$(see Appendix A):

$$\mathfrak{a}(\Omega) = \frac{a(\omega_0 + \Omega) + a^\dagger(\omega_0 - \Omega)}{\sqrt{2}},$$

Without the loss of generality we assume that $\mathcal{A}/\mathcal{T}_{\delta_1}^2 = \mathcal{B}/\mathcal{T}_{\delta_2}^2$ and both are pure real; this assumption significantly simplifies all the calculations and can be easily realized in practice by special choice of amplitudes and phases of $\mathcal{A}$ and $\mathcal{B}$. Then the cosine quadratures corresponding to the fields (16a – 16d) are:

$$\begin{aligned}
\mathfrak{a}^{\rm r}_{\rm out} &= \frac{\mathcal{R}_1 a_{\rm in} + \mathcal{R}^*_{1-} a^\dagger_{\rm in-}}{\sqrt{2}} + \frac{\mathcal{T}_1 a_{\rm vac} + \mathcal{T}^*_{1-} a^\dagger_{\rm vac-}}{\sqrt{2}} \\
&\quad + \frac{\mathcal{A}}{\mathcal{T}_{\delta_1}^2}\,\sqrt{2}ik_0\Big[\alpha_1(\xi_b + \xi_{\rm gw})e^{i\Omega\tau} - \beta_1\xi_a\Big], \\
\mathfrak{a}^{\rm t}_{\rm out} &= \frac{\mathcal{T}_1 a_{\rm in} + \mathcal{T}^*_{1-} a^\dagger_{\rm in-}}{\sqrt{2}} + \frac{\mathcal{R}_1 a_{\rm vac} + \mathcal{R}^*_{1-} a^\dagger_{\rm vac-}}{\sqrt{2}} \\
&\quad + \frac{\mathcal{A}}{\mathcal{T}_{\delta_1}^2}\,\sqrt{2}ik_0\Big[\gamma_1(\xi_b + \xi_{\rm gw})e^{2i\Omega\tau} - \gamma_1\xi_a e^{i\Omega\tau}\Big], \\
\mathfrak{b}^{\rm r}_{\rm out} &= \frac{\mathcal{R}_2 b_{\rm in} + \mathcal{R}^*_{2-} b^\dagger_{\rm in-}}{\sqrt{2}} + \frac{\mathcal{T}_2 b_{\rm vac} + \mathcal{T}^*_{2-} b^\dagger_{\rm vac-}}{\sqrt{2}} \\
&\quad + \frac{\mathcal{B}}{\mathcal{T}_{\delta_2}^2}\,\sqrt{2}ik_0\Big[\alpha_2(-\xi_a + \xi_{\rm gw})e^{i\Omega\tau} + \beta_2\xi_b\Big], \\
\mathfrak{b}^{\rm t}_{\rm out} &= \frac{\mathcal{T}_2 b_{\rm in} + \mathcal{T}^*_{2-} b^\dagger_{\rm in-}}{\sqrt{2}} + \frac{\mathcal{R}_2 b_{\rm vac} + \mathcal{R}^*_{2-} b^\dagger_{\rm vac-}}{\sqrt{2}} \\
&\quad + \frac{\mathcal{B}}{\mathcal{T}_{\delta_2}^2}\,\sqrt{2}ik_0\Big[\gamma_2(-\xi_a + \xi_{\rm gw})e^{2i\Omega\tau} + \gamma_2\xi_b e^{i\Omega\tau}\Big],
\end{aligned}$$

where

$$\begin{aligned}
\alpha_j(\Omega) &= -\frac{RT^2}{\mathfrak{T}_j}\,2i\sin 2\delta_j\tau, \\
\beta_j(\Omega) &= \frac{R^3}{\mathfrak{T}_j}\,2i\sin 2\delta_j\tau\big(1 - 2e^{2i\Omega\tau}\cos 2\delta_j\tau + R^2e^{4i\Omega\tau}\big), \\
\gamma_j(\Omega) &= \frac{R^2T^2}{\mathfrak{T}_j}\,2i\big(\sin 3\delta_j\tau - R^2e^{2i\Omega\tau}\sin\delta_j\tau\big), \\
\mathfrak{T}_j(\Omega) &= \mathcal{T}^2_{\delta_j+\Omega}\big(\mathcal{T}^2_{\delta_j-\Omega}\big)^*.
\end{aligned}$$

and $\mathcal{R}^*_{j-} = \mathcal{R}^*_j(-\Omega)$, $\mathcal{T}^*_{j-} = \mathcal{T}^*_j(-\Omega)$ for $j = 1, 2$ and $a^\dagger_- = a^\dagger(\omega_j - \Omega)$. Now we perform the three-steps algorithm in order to cancel the displacement noise:

$$\begin{aligned}
\mathfrak{s}_1 &= \mathfrak{a}^{\rm r}_{\rm out}e^{i\Omega\tau} - (\beta_1/\gamma_1)\mathfrak{a}^{\rm t}_{\rm out} \\
&= \mathfrak{s}^{\rm fl}_1 + \frac{\mathcal{A}}{\mathcal{T}_{\delta_1}^2}\,\sqrt{2}ik_0(\alpha_1 - \beta_1)(\xi_b + \xi_{\rm gw})e^{2i\Omega\tau}, \\
\mathfrak{s}_2 &= \mathfrak{b}^{\rm r}_{\rm out}e^{i\Omega\tau} - (\alpha_2/\gamma_2)\mathfrak{b}^{\rm t}_{\rm out} \\
&= \mathfrak{s}^{\rm fl}_2 - \frac{\mathcal{B}}{\mathcal{T}_{\delta_2}^2}\,\sqrt{2}ik_0(\alpha_2 - \beta_2)\xi_b e^{i\Omega\tau}, \\
\mathfrak{s} &= \mathfrak{s}_1 + \frac{\alpha_1 - \beta_1}{\alpha_2 - \beta_2}\,\mathfrak{s}_2 e^{i\Omega\tau}
\end{aligned}$$

$$= \mathfrak{s}^{\rm fl} + \frac{\mathcal{A}}{\mathcal{T}_{\delta_1}^2}\sqrt{2}ik_0(\alpha_1-\beta_1)\xi_{\rm gw}e^{2i\Omega\tau},$$

where $\alpha_1-\beta_1 = -2iR\sin 2\delta_1\tau$. Obviously, the difference $\alpha_1-\beta_1$ plays the key role: the larger it is, the larger is the DFI signal. In narrow-band and low-frequency approximations $\alpha_1-\beta_1 \approx -4i\delta_1\tau$ and

$$\mathfrak{s} \approx \mathfrak{s}^{\rm fl} + \frac{\delta_1}{\gamma-i\delta_1}\,\mathcal{A}\sqrt{2}k_0Lh, \tag{22}$$

with $\mathcal{A}\delta/(\gamma-i\delta)\in\mathbb{R}$.

Terms $\mathfrak{s}_1^{\rm fl}$, $\mathfrak{s}_2^{\rm fl}$ and $\mathfrak{s}^{\rm fl}$ correspond to the optical shot noise and have a complicated dependence on δ_1, δ_2 and Ω in general case; they can be calculated explicitly in the most interesting case of narrow-band and low-frequency approximations when $\alpha_i\approx\beta_i\approx-\gamma_i$ and $\mathcal{R}_i+\mathcal{T}_i\approx 1$:

$$\begin{aligned}
\mathfrak{s}_1^{\rm fl} \approx& \frac{(\mathcal{R}_1+\mathcal{T}_1)(a_{\rm in}+a_{\rm vac})}{\sqrt{2}}\\
&+\frac{(\mathcal{R}_{1-}^*+\mathcal{T}_{1-}^*)(a_{\rm in-}^\dagger+a_{\rm vac-}^\dagger)}{\sqrt{2}} \approx \mathfrak{a}_{\rm in}+\mathfrak{a}_{\rm vac},\\
\mathfrak{s}_2^{\rm fl} \approx& \frac{(\mathcal{R}_2+\mathcal{T}_2)(b_{\rm in}+b_{\rm vac})}{\sqrt{2}}\\
&+\frac{(\mathcal{R}_{2-}^*+\mathcal{T}_{2-}^*)(b_{\rm in-}^\dagger+b_{\rm vac-}^\dagger)}{\sqrt{2}} \approx \mathfrak{b}_{\rm in}+\mathfrak{b}_{\rm vac}.
\end{aligned}$$

Remind that $\mathfrak{a}_{\rm in} = (a_{\rm in}+a_{\rm in-}^\dagger)/\sqrt{2}$ and so on.

In the case of equal detunings ($\delta_2=\delta_1$) we have $\alpha_2=\alpha_1$ and $\beta_2=\beta_1$. Therefore, $\mathfrak{s}^{\rm fl}=\mathfrak{s}_1^{\rm fl}+\mathfrak{s}_2^{\rm fl}$ and

$$\mathfrak{s}|_{\delta_2=\delta_1} \approx \mathfrak{a}_{\rm in}+\mathfrak{b}_{\rm in}+\mathfrak{a}_{\rm vac}+\mathfrak{b}_{\rm vac}+\frac{\delta_1}{\gamma-i\delta_1}\,\mathcal{A}\sqrt{2}k_0Lh.$$

In the case of opposite detunings ($\delta_2=-\delta_1$) we have $\alpha_2=-\alpha_1$ and $\beta_2=-\beta_1$. Therefore, $\mathfrak{s}^{\rm fl}=\mathfrak{s}_1^{\rm fl}-\mathfrak{s}_2^{\rm fl}$ and

$$\mathfrak{s}|_{\delta_2=-\delta_1} \approx \mathfrak{a}_{\rm in}-\mathfrak{b}_{\rm in}+\mathfrak{a}_{\rm vac}-\mathfrak{b}_{\rm vac}+\frac{\delta_1}{\gamma-i\delta_1}\,\mathcal{A}\sqrt{2}k_0Lh.$$

Note that in the case of the sine quadratures the GW-term in the sine DFI response signal is $\delta_1\tau$ times weaker than the one in signal (22). However, for completeness we present detailed calculations for the sine quadratures in Appendix D.

IV. DISCUSSION

A. Physical mechanism of noise cancelation

Due to the (weak) equivalence principle it is possible to construct the local Lorentz frame for a test mass in which the latter becomes free-falling and hence does not sense the gravitational wave. In our case we constructed such a reference frame for mirror a (in the case of pump through that mirror) and thus isolated it from the influence of a GW (see formulas (14a, 14b)). This in turn allowed us to separate the GW signal $\xi_{\rm gw}$ from the fluctuating displacement ξ_a of that mirror (see formulas (16a, 16b)). In the case of pump through mirror b the situation is similar: we work in the local Lorentz frame of this mirror and separate the GW signal $\xi_{\rm gw}$ from its fluctuating displacement ξ_b (see formulas (16c, 16d)).

The separation of the GW signal from fluctuating displacements can also be interpreted in the following way. In the transverse-traceless (TT) gauge the space-time of GW manifests itself as the medium with effective refraction index; during one round trip in this medium along the interferometer arm the light wave accumulates phase shift equal to $2k_0\xi_{\rm gw}(\Omega)$ in spectral domain. Obviously, in this description the effective optical properties of the medium (distributed effect) are independent of the fluctuations of the test masses (localized effect) and should enter the response signals separately.

Note that this feature does not hold true if the test masses move in the force-field not obeying the equivalence principle (GW is absent). Let us assume we want to perform the displacement-noise-free measurement of that force with the DPFP cavity using the algorithm described in Sec. III B. In this case we are no longer able to construct the locally inertial reference frame for any of the test masses and are forced to work in the laboratory frame. Let for definiteness consider the external non-gravitational force $\mathbf{F}(t)$ acting on mirror b along the x-axis. We denote the corresponding displacement of the mirror as ξ_F. Then, neglecting all the unnecessary terms, we would obtain from formulas (16a – 16d) in the simplest case of equal pumps:

$$\begin{aligned}
a_{\rm out}^{\rm r} \sim& (\xi_b+\xi_F)e^{i\Omega\tau}-\sigma\xi_a,\\
a_{\rm out}^{\rm t} \sim& (\xi_b+\xi_F)e^{2i\Omega\tau}-\xi_a e^{i\Omega\tau},\\
b_{\rm out}^{\rm r} \sim& -\xi_a e^{i\Omega\tau}+\sigma(\xi_b+\xi_F),\\
b_{\rm out}^{\rm t} \sim& -\xi_a e^{2i\Omega\tau}+(\xi_b+\xi_F)e^{i\Omega\tau}.
\end{aligned}$$

Note that the force-induced displacement ξ_F cannot be separated from ξ_b in all the output signals. It is straightforward to verify now that performing the three steps similar to (17 – 19) to cancel fluctuations $\xi_{a,b}$ we would come to $s\equiv 0$.

The same holds true for the force of interaction between the mirrors, i.e. $\mathbf{F}(t)=\mathbf{F}(|x_a-x_b|,\,t)$. In this case, assuming equal masses of the mirrors:

$$\begin{aligned}
a_{\rm out}^{\rm r} \sim& (\xi_b+\xi_F)e^{i\Omega\tau}-\sigma(\xi_a-\xi_F),\\
a_{\rm out}^{\rm t} \sim& (\xi_b+\xi_F)e^{2i\Omega\tau}-(\xi_a-\xi_F)e^{i\Omega\tau},\\
b_{\rm out}^{\rm r} \sim& (-\xi_a+\xi_F)e^{i\Omega\tau}+\sigma(\xi_b+\xi_F),\\
b_{\rm out}^{\rm t} \sim& (-\xi_a+\xi_F)e^{2i\Omega\tau}+(\xi_b+\xi_F)e^{i\Omega\tau},
\end{aligned}$$

and again after cancelation of displacement noise we come to $s\equiv 0$.

Therefore, we conclude that in our case one of the key roles in isolation of the GW signal from displacement noise is played by the equivalence principle in terms of

the LL gauge or by the distributed nature of GWs in terms of the TT gauge.

Furthermore, the proportionality of the DFI signal (19) to the detuning from resonance $1-e^{2i\delta_1\tau}$ implies that no cancelation of noise is possible at resonance. The reason for this is the following. It is straightforward to verify using formulas (15a, 15b) that in the resonant regime ($\delta_1 = 0$, $\Delta\sigma_1 = 0$) the response signals (neglecting the optical noise terms) of a FP cavity obey the relation $a^{\rm t}_{\rm out} = Ra^{\rm r}_{\rm out}e^{i\Omega\tau}$ or $a^{\rm t}_{\rm out}(t) = Ra^{\rm r}_{\rm out}(t-\tau)$ and therefore, carry equal amount of information about the GW signal and displacement noise. Thus we cannot cancel any fluctuating coordinate using their linear combination since it erases the information about all the $N \approx 1/(2\gamma\tau)$ photon round trips inside the cavity (see formula (17)).

Signals $a^{\rm r}_{\rm out}$ and $a^{\rm t}_{\rm out}$ (and similar $b^{\rm r,t}_{\rm out}$) become different only in the non-resonant regime with the difference described by factor $\Delta\sigma_1$ ($\Delta\sigma_2$ for $b^{\rm r,t}_{\rm out}$). Then their proper linear combination partially cancels the information about N photon round trips, leaving a non-vanishing part proportional to $\Delta\sigma_1$ ($\Delta\sigma_2$ for $b^{\rm r,t}_{\rm out}$). Therefore, another key role in the cancelation of displacement noise is played by the asymmetry between the reflection and transmission ports of the detuned cavity.

The loss of the information about round trips results in the loss of the optical resonant gain described by the $1/\mathcal{T}^2_{\omega_0+\Omega}$-multiplier. That is the "payment" for isolation of the GW signal from displacement noise in our case.

Note also that the direct coupling of the GW to the light wave in the LL gauge, i.e. phase shift (12), plays no role in our noise-cancelation scheme: it could be omitted from the beginning since the leading order effect is $h(L/\lambda_{\rm gw})^0$. In other words, the notion of the GW in all the presented considerations can be approximated with the corresponding tidal force-field. In terms of the TT gauge this means that the difference between the localized nature of displacement noise and the distributed nature of GWs is utilized in a DPFP cavity in another way compared to the DFIs in Refs. [27–29]. Namely, Y. Chen's *et al.* noise-cancelation schemes utilize the $h(L/\lambda_{\rm gw})^n$-terms with $n \geq 2$ which are the measure of the asymmetry between the GWs and the external forces, while our algorithm utilizes the asymmetry between the output ports of the cavity (with the measure of the asymmetry $|\Delta\sigma| \approx \delta\tau$) and hence does not rely on the cancelation of the $h(L/\lambda_{\rm gw})^0$-term. The difference between the GWs and the external forces in our case plays the role of the necessary condition of obtaining of a non-trivial result after performing the noise-cancelation algorithm (see discussion of the displacement-noise-free measurement of an external force above).

B. DPFP cavity compared to Mach-Zehnder-based DFIs and conventional interferometers

Let us compare the DPFP cavity with the Mach-Zehnder-based DFIs proposed in Ref. [29] in the most important, low-frequency, part of the spectrum. We assume that the laser noise is somehow canceled in a DPFP cavity (see Sec. IV C).

According to formulas (20, 21) for $\gamma \sim \delta$ the GW response function has the numerical multiplier $i\delta/(\gamma - i\delta)$ of the order of unity. This can be compared to the $(\Omega\tau)^3$-limited sensitivity of the two-dimensional double-Mach-Zehnder topology. For $\Omega/2\pi \approx 100$ Hz and $\tau = L/c \approx 10^{-5}$ s we have $(\Omega\tau)^3 \sim 2\times 10^{-7}$. However, the level of shot noise is approximately identical for both the DPFP and MZ topologies. Therefore, the signal-to-noise ratio of the DPFP cavity is far better than that of the MZ configurations. The difference in their sensitivities arises due to the different mechanisms of displacement noise cancelation as discussed above.

Note that from the point of view of the shot noise-limited sensitivity the DPFP cavity is no better or worse than a simple one-round-trip detector.

In conventional LIGO (Michelson/Fabry-Perot) topology optical cavities are utilized to accumulate the low-frequency signals with the corresponding resonant gain having the order of $(\gamma\tau)^{-1}$, where γ is the cavity half-bandwidth. For $\gamma/2\pi \approx \Omega/2\pi \approx 100$ Hz and $\tau = L/c \approx 10^{-5}$ we have $(\gamma\tau)^{-1} \sim 10^2$. However, the level of shot noise is still approximately equal to the one of the DPFP cavity. Therefore, the latter is $\sim 10^2$ times worse in the shot noise-limited sensitivity than current (and planned) GW detectors. Nevertheless, the main feature making the DPFP cavity a promising candidate for the 3rd generation prototypes is the invulnerability to the Standard Quantum Limit since radiation pressure noise, responsible for back-action noise, is canceled. In addition, it allows the significant extension of the frequency band of the Earth-based detectors: beginning from ~ 50 Hz current detectors are limited by seismic and gravity-gradient noise (the so-called seismic wall), while the displacement-noise-free detectors will be free from this limitation.

C. Further prospects: cancelation of laser noise and radiation pressure effects

In practice laser noise dominates over vacuum shot noise. In addition, as pointed out in Ref. [28], laser noise is indistinguishable from displacement noise. Therefore, in order to perform a complete displacement-noise-free GW detection we should somehow eliminate the laser noise. Several obvious DPFP-based laser-noise-cancelation schemes can be proposed [51]: (i) with a single DPFP cavity where both the pumps are generated with a single laser and one of the pumps is redirected towards mirror b via additional optical path, (ii) with a pair of parallel and closely located DPFP cavities having different bandwidths and/or detunings, (iii) modification of the conventional LIGO Michelson/Fabry-Perot topology, etc. However, the major drawback of all such schemes is the significant amount of the additional optical elements such as beamsplitters and mirrors which

are utilized to split and redirect laser beams. These elements introduce the additional displacement noise with the magnitude compared to the GW signal $k_0 Lh$. In conventional interferometers (such as LIGO) this additional noise is negligible compared to the (FP cavity) finesse times amplified GW signal (and mirrors displacement noise), while the DPFP cavity operating in the DFI regime effectively "loses" the resonant gain as discussed in Sec. IV A. Therefore, the problem of additional displacement noise requires a separate detailed analysis and it may turn out that it will be highly suppressed after performing the noise-cancelation algorithm described in Sec. III B.

The related problem is the construction of the experimentally viable and most practical measurement schemes. In particular, in this paper we assumed all the optical elements (mirrors, beamsplitters, photodetectors) on platforms P_1 and P_2 to be noiseless (i.e. rigidly installed). In practice this assumption may be hard to justify and thus requires further intensive study. Moreover, the implementation of the scheme for detecting the transmitted waves (considered in this paper) with the local oscillator and the homodyne detector located on different platforms (such as in Fig. 2), separated by a kilometer-scale distance, can be complicated in practice. Thus the configuration with the co-located local oscillator and the homodyne detector requires a separate analysis.

Furthermore, in this paper we have deliberately ignored the role of radiation pressure effects emerging in the non-resonant FP cavity. According to the analysis performed in Ref. [37], the motion of test mass m under the influence of weak external force $F(t)$ in the field of weak plane gravitational wave $h(t)$ will obey the following equation of motion in the first order:

$$m\left[\frac{d^2X}{dt^2} - \frac{1}{2}L\ddot{h}(t)\right] = F(t)$$

If $F(t)$ is the ponderomotive part of the radiation pressure force [42–46] having the Fourier image $F(\Omega) = -K(\Omega)X(\Omega)$, where $K(\Omega)$ is the coefficient of optical rigidity [37], then we come to the following law of motion (in long-wave approximation $\Omega\tau \ll 1$):

$$X(\Omega) = \frac{m\Omega^2}{m\Omega^2 - K(\Omega)}\,\frac{1}{2}\,Lh(\Omega).$$

Assume now that in a detuned FP cavity with both movable mirrors ponderomotive force equals to $F = -K(X_b - X_a)$ (this assumption must be carefully verified). Then taking into account formulas (14a, 14b) we should replace in response signals (16a – 16d)

$$\xi_{\rm gw} \to \frac{m\Omega^2}{m\Omega^2 - K(\Omega)}\,\xi_{\rm gw}.$$

At certain frequencies one can achieve the condition of optomechanical resonance $m\Omega^2 - \Re(K) = 0$ [47–50], thus further amplifying the displacement-noise-free response of the DPFP cavity. It should be stressed, however, that the radiation pressure effects also require a separate analysis [51].

V. CONCLUSION

In this paper we have analyzed the operation of a Fabry-Perot cavity pumped through both the mirrors (a DPFP cavity) performing the displacement-noise-free gravitational-wave detection. We have demonstrated that due to the asymmetry between the reflection and transmission output ports of the detuned cavity it is possible to construct such a linear combination of four response signals which cancels displacement fluctuations of the test masses. At low frequencies the signal-to-noise ratio of the shot noise-limited DPFP cavity turns out to be far better than that of the Mach-Zehnder-based DFIs proposed by Y. Chen *et al.* due to the different mechanisms of noise-cancelation.

The performed analysis suggests that the DPFP cavity can be considered a promising candidate for the 3rd generation detector prototype: it allows the significant extension of the frequency band of the ground-based detectors and by elimination of the back-action noise straightforwardly avoids the standard quantum limitation.

The problems of (i) constructing the DPFP-based laser-noise-cancelation schemes and (ii) the radiation pressure effects in a DPFP cavity require future investigation.

Acknowledgments

We are grateful to V.B. Braginsky, M.L. Gorodetsky and F.Ya. Khalili for fruitful discussion and valuable critical remarks. This work was supported by LIGO team from Caltech and in part by NSF and Caltech grant PHY-0353775 and by Grant of President of Russian Federation NS-5178.2006.2.

APPENDIX A: QUANTIZED ELECTROMAGNETIC WAVE

In this Appendix we introduce the notations for the quantized field of electromagnetic wave which will be used throughout the paper.

In quantum electrodynamics the operator of electric field in Heisenberg picture is:

$$A(x,t) = \int_0^\infty \sqrt{\frac{2\pi\hbar\omega}{Sc}}\,a(\omega)e^{-i\omega(t-x/c)}\,\frac{d\omega}{2\pi} + \text{h.c.},$$

where S is the effective cross section area of the laser beam and $a(\omega)$ is the annihilation operator obeying the commutation relations

$$\left[a(\omega), a(\omega')\right] = 0, \quad \left[a(\omega), a^\dagger(\omega')\right] = 2\pi\delta(\omega - \omega').$$

It will be convenient now to introduce the carrier frequency ω_0: $\omega = \omega_0 + \Omega$, $|\Omega| \ll \omega_0$, and to rewrite the field operator in the following way:

$$A(x,t) = e^{-i(\omega_0 t - k_0 x)} \times \int_{-\omega_0}^{\infty} \sqrt{\frac{2\pi\hbar(\omega_0+\Omega)}{Sc}}\, a(\omega_0+\Omega) e^{-i\Omega(t-x/c)}\, \frac{d\Omega}{2\pi} + \text{h.c.},$$

where $k_0 = \omega_0/c$. Now we split the annihilation operator into two summands:

$$a(\omega_0+\Omega) = A_0\delta(0) + a'(\omega_0+\Omega).$$

For convenience we change notation $a' \to a$ since we do not need old a any further. Extending now the lower limit of integration to $-\infty$ (since $|\Omega| \ll \omega_0$), we finally obtain the double-sided (from $-\infty$ to $+\infty$) expression for the field operator:

$$A(x,t) = \sqrt{\frac{2\pi\hbar\omega_0}{Sc}}\, e^{-i(\omega_0 t - k_0 x)} \times \left[A_0 + \int_{-\infty}^{+\infty} a(\omega_0+\Omega) e^{-i\Omega(t-x/c)}\, \frac{d\Omega}{2\pi}\right] + \text{h.c.} \tag{A1}$$

In these notations electric field of the wave is represented as a sum of (i) "strong" (classical) wave with amplitude A_0 and (carrier) frequency ω_0 and (ii) "weak" wave describing the quantum fluctuations of the optical field with its amplitude obeying the commutation relations:

$$\left[a(\omega_0+\Omega), a(\omega_0+\Omega')\right] = 0,$$
$$\left[a(\omega_0+\Omega), a^\dagger(\omega_0+\Omega')\right] = 2\pi\delta(\Omega-\Omega').$$

The double-sided expression is the one most close to the Fourier representation of the classical fields and will be used throughout the paper. For convenience we omit the $\sqrt{2\pi\hbar\omega_0/Sc}$-multiplier in the main body of the paper since it is the common multiplier in all the equations.

In Sec. III we deal with the quadrature components of the wave which are introduced in the following way.

Formula (A1) can be rewritten as:

$$A(x,t) = \sqrt{\frac{2\pi\hbar\omega_0}{Sc}}\, e^{-i(\omega_0 t - k_0 x)} \times \left\{A_0 + \int_0^{\infty} \left[a_{\omega_0+\Omega} e^{-i\Omega(t-x/c)} + a_{\omega_0-\Omega} e^{i\Omega(t-x/c)}\right] \frac{d\Omega}{2\pi}\right\} + \text{h.c.}, \tag{A2}$$

where $a_{\omega_0-\Omega}$ obeys the same commutation relation as $a_{\omega_0+\Omega}$:

$$[a_{\omega_0+\Omega}, a^\dagger_{\omega_0+\Omega'}] = [a_{\omega_0-\Omega}, a^\dagger_{\omega_0-\Omega'}] = 2\pi\delta(\Omega-\Omega').$$

Next we introduce the so-called correlated two-photon modes with field operators [54, 55]

$$a_{\rm c}(\Omega) = \frac{a_{\omega_0+\Omega} + a^\dagger_{\omega_0-\Omega}}{\sqrt{2}}, \qquad a_{\rm s}(\Omega) = \frac{a_{\omega_0+\Omega} - a^\dagger_{\omega_0-\Omega}}{\sqrt{2}i},$$

with the only non-zero commutators

$$[a_{\rm c}, a^\dagger_{\rm s'}] = [a_{\rm c'}, a^\dagger_{\rm s}] = 2\pi i\delta(\Omega-\Omega'),$$

where prime denotes the argument with Ω'. In terms of these two-photon modes formula (A2) takes the form:

$$A(x,t) = \sqrt{\frac{4\pi\hbar\omega_0}{Sc}} \Big[\sqrt{2}A_0\cos(\omega_0 t - k_0 x) + a_{\rm c}(x,t)\cos(\omega_0 t - k_0 x) + a_{\rm s}(x,t)\sin(\omega_0 t - k_0 x)\Big], \tag{A3}$$

where operators

$$a_{\rm c}(x,t) = \int_0^{\infty} \left[a_{\rm c}(\Omega) e^{-i\Omega(t-x/c)} + a^\dagger_{\rm c}(\Omega) e^{i\Omega(t-x/c)}\right] \frac{d\Omega}{2\pi}, \tag{A4a}$$

$$a_{\rm s}(x,t) = \int_0^{\infty} \left[a_{\rm s}(\Omega) e^{-i\Omega(t-x/c)} + a^\dagger_{\rm s}(\Omega) e^{i\Omega(t-x/c)}\right] \frac{d\Omega}{2\pi}, \tag{A4b}$$

in the case $A_0 = 0$ are called the cosine and sine quadratures (or quadrature components) correspondingly.

We will also need the double-sided expressions of the quadratures which are obtained from formulas (A4a), A4b) and conditions $a_{\rm c,s}(\Omega) = a^\dagger_{\rm c,s}(-\Omega)$:

$$a_{\rm c}(x,t) = \int_{-\infty}^{+\infty} a_{\rm c}(\Omega) e^{-i\Omega(t-x/c)}\, \frac{d\Omega}{2\pi},$$
$$a_{\rm s}(x,t) = \int_{-\infty}^{+\infty} a_{\rm s}(\Omega) e^{-i\Omega(t-x/c)}\, \frac{d\Omega}{2\pi}.$$

APPENDIX B: SCHEME FOR MEASURING THE RESPONSE SIGNALS

In this Appendix we analyze explicitly the measurement of the quadrature components of the cavity response signals $a^{\rm r}$ and $a^{\rm t}$ (formulas (11a) and (11b) correspondingly). In particular we will consider the case of the transmitted output wave since it raises a greater amount of problems rather than the reflected signal. With corresponding replacements the following analysis remains valid for the case of a double-pumped FP cavity.

Assume that laser L pumps a FP cavity through mirror a and transmitted wave $A^{\rm t}_{\rm out}(x,t)$ is detected (see Figs. 1 and 2). Remind, that the measurement scheme assembled on platform $\rm P_2$ is the absolutely rigid body. Let us assume that the coordinate of platform $\rm P_2$ (its center of mass for definiteness) is $x_{\rm P_2} = L + l_{\rm P_2} + X_{\rm P_2}$, with $l_{\rm P_2}, X_{\rm P_2} \ll L$. Here $l_{\rm P_2}$ is the distance between mirror b and the center of mass of platform $\rm P_2$ in the state of rest; $X_{\rm P_2}$ is the displacement of platform $\rm P_2$ from the position of equilibrium. It is worth noting that displacement $X_{\rm P_2}$, apart from displacement fluctuation of the platform $\xi_{\rm P_2}$, contains the GW signal due to the account of the tidal

displacement $\frac{1}{2}Lh(t)$ in the LL gauge since $l_{\mathrm{P}_2} \ll L$ (see formula (14b)).

Then according to formula (9) in the LL gauge we obtain the following transmitted wave at point $x = x_{\mathrm{P}_2}$:

$$A^{\mathrm{t}}_{\mathrm{out}}(x_{\mathrm{P}_1}, t) = A^{\mathrm{t}}_{\mathrm{out}0}\Big[1 + g_+(L,t)\Big]e^{-i\omega_1 t + ik_1(l_{\mathrm{P}_2}+X_{\mathrm{P}_2})} + a^{\mathrm{t}}_{\mathrm{out}}(L,t)e^{-i\omega_1 t + ik_1(l_{\mathrm{P}_2}+X_{\mathrm{P}_2})}, \quad \text{(B1)}$$

with

$$A^{\mathrm{t}}_{\mathrm{out}0} = \frac{T^2 e^{i\omega_1\tau}}{1 - R^2 e^{2i\omega_1\tau}}\, A_{\mathrm{in}0} \approx A_{\mathrm{in}0} e^{i\omega_1\tau}.$$

In order to measure the quadrature components of $a^{\mathrm{t}}_{\mathrm{out}}(L,t)$ we must perform a balanced homodyne detection. To do this we need some reference oscillation (a local oscillator, LO) with big amplitude and variable phase. Such a reference oscillation can be produced by the pump wave from laser L (with much greater amplitude than the one of the wave incident on mirror a of the cavity) passing through the phase shifter Φ_2. Then the reference oscillation at point $x = x_{\mathrm{P}_2}$ according to formula (5) is:

$$A_{\mathrm{LO}}(x_{\mathrm{P}_1}, t) = A_{\mathrm{LO}0}\Big[1 + g_+(L,t)\Big]e^{-i\omega_1 t + ik_1(l_{\mathrm{P}_2}+X_{\mathrm{P}_2}) - i\Theta} + a_{\mathrm{LO}}(L,t)e^{-i\omega_1 t + ik_1(l_{\mathrm{P}_2}+X_{\mathrm{P}_2}) - i\Theta}, \quad \text{(B2)}$$

where $|A_{\mathrm{LO}0}| \gg |A_{\mathrm{in}0}|$, $\Theta = \theta - \omega_1\tau$ and θ is the phase shift induced by the phase shifter Φ_2.

This reference oscillation also allows us to take into account the effect of localized redshift discussed in Ref. [36]: if in the local Lorentz gauge the phase of the signal wave (transmitted wave in our case) is measured, i.e. compared to the phase of the reference oscillation, at point $x_0 \neq 0$ then the reference oscillation must be defined with respect to the local time $t^* = \int dt\sqrt{-g_{00}(x_0,t)}$.

Note that in both the formulas (B1) and (B2) we should have taken the fluctuating displacement X_{P_1} of platform P_1 into account since the phase shift accumulated by the light wave along the optical path $\mathrm{M}_1\mathrm{M}_2$ (see Fig. 2) is proportional to $|x_{\mathrm{P}_2} - x_{\mathrm{P}_1}| \approx |L + X_{\mathrm{P}_2} - X_{\mathrm{P}_1}|$. However, displacement noise of platform P_1 (and hence of laser L) can be included in the definition of the optical laser noise a_{in} or a_{LO} as the term proportional to $A_{\mathrm{in}0}ik_1X_{\mathrm{P}_1}$ or $A_{\mathrm{LO}0}ik_1X_{\mathrm{P}_1}$ correspondingly.

Let the beamsplitter BS_2 have transmittance and reflectivity both equal to $1/\sqrt{2}$. Then photodetector PhD_3 produces photocurrent J_3 proportional to $|A^{\mathrm{t}}_{\mathrm{out}}(x_{\mathrm{P}_2},t) + A_{\mathrm{LO}}(x_{\mathrm{P}_2},t)|^2/2$ and photodetector PhD_4 produces photocurrent J_4 proportional to $|A^{\mathrm{t}}_{\mathrm{out}}(x_{\mathrm{P}_2},t) - A_{\mathrm{LO}}(x_{\mathrm{P}_2},t)|^2/2$. In an explicit form this can be written as:

$$J_3 \propto \frac{1}{2}\Big|A^{\mathrm{t}}_{\mathrm{out}0}\Big[1 + g_+(L,t)\Big] + a^{\mathrm{t}}_{\mathrm{out}}(L,t) + A_{\mathrm{LO}0}e^{-i\Theta}\Big[1 + g_+(L,t)\Big] + a_{\mathrm{LO}}(L,t)e^{-i\Theta}\Big|^2,$$

and

$$J_4 \propto \frac{1}{2}\Big|A^{\mathrm{t}}_{\mathrm{out}0}\Big[1 + g_+(L,t)\Big] + a^{\mathrm{t}}_{\mathrm{out}}(L,t) - A_{\mathrm{LO}0}e^{-i\Theta}\Big[1 + g_+(L,t)\Big] - a_{\mathrm{LO}}(L,t)e^{-i\Theta}\Big|^2.$$

Here for simplicity we consider classical waves and complex conjugates instead of Hermitian conjugates. Note that both the fluctuating and GW displacements (ξ_{P_2} and $\frac{1}{2}Lh$ correspondingly) of platform P_2 included in X_{P_2} are canceled from both the currents.

It is straightforward to verify that the differential current in subtractor S_2 is:

$$\begin{aligned}\Delta J &= J_3 - J_4\\ &\sim 2\Big[(A^{\mathrm{t}}_{\mathrm{out}0})^* a_{\mathrm{LO}}e^{-i\Theta} + A^{\mathrm{t}}_{\mathrm{out}0}(a_{\mathrm{LO}})^* e^{i\Theta}\Big]\\ &+ 2\Big[(A_{\mathrm{LO}0})^* e^{i\Theta}a^{\mathrm{t}}_{\mathrm{out}} + A_{\mathrm{LO}0}e^{-i\Theta}(a^{\mathrm{t}}_{\mathrm{out}})^*\Big]\\ &+ 2\Big[(A^{\mathrm{t}}_{\mathrm{out}0})^* A_{\mathrm{LO}0}e^{-i\Theta} + A^{\mathrm{t}}_{\mathrm{out}0}(A_{\mathrm{LO}0})^* e^{i\Theta}\Big](g_+ + g_+^*),\end{aligned}$$

where for briefness we omitted the (L,t) arguments. Note that due to the inequality $|A_{\mathrm{LO}0}| \gg |A_{\mathrm{in}0}|$ we have $|A^{\mathrm{t}}_{\mathrm{out}0}| \ll |A_{\mathrm{LO}0}|$ and thus the first summand in ΔJ can be omitted. Moreover, due to formulas (3b, 3c)

$$\begin{aligned}&g_+(L,t) + g_+^*(L,t)\\ &= \int_{-\infty}^{+\infty}\Big[g_+(L,\omega_0+\Omega) + g_+^*(L,\omega_0-\Omega)\Big]e^{-i\Omega t}\,\frac{d\Omega}{2\pi} \equiv 0,\end{aligned}$$

and the third summand in ΔJ vanish identically. Assuming now $A_{\mathrm{LO}0} \in \mathbb{R}$ we obtain the usual formula for the homodyne current:

$$\Delta J \sim 2A_{\mathrm{LO}0}\Big[a^{\mathrm{t}}_{\mathrm{out}}e^{i\Theta} + (a^{\mathrm{t}}_{\mathrm{out}})^* e^{-i\Theta}\Big].$$

In the case of measuring the reflected signal $A^{\mathrm{t}}_{\mathrm{out}}(x,t)$ all the formulas become simpler. In particular, if we measure the reflected signal at point $x = x_{\mathrm{P}_1} \approx 0$ then the $g_\pm$-terms vanish from the beginning since $g_\pm(0,t) \equiv 0$.

APPENDIX C: BOUNDARY CONDITIONS

In this Appendix we solve the set of equations (10a – 10d).

First we substitute fields (5 – 9) into this set and separate the zeroth and the first order sets.

The zeroth order set is:

$$\begin{aligned}A_{+0} &= TA_{\mathrm{in}0} - RA_{-0},\\ A^{\mathrm{r}}_{\mathrm{out}0} &= RA_{\mathrm{in}0} + TA_{-0},\\ A_{-0} &= -RA_{+0}e^{2i\omega_1\tau},\\ A^{\mathrm{t}}_{\mathrm{out}0} &= TA_{+0}e^{i\omega_1\tau}.\end{aligned}$$

Corresponding solution is:

$$A_{+0} = \frac{T}{1-R^2e^{2i\omega_1\tau}}\,A_{\rm in0},$$
$$A_{-0} = -\frac{RTe^{2i\omega_1\tau}}{1-R^2e^{2i\omega_1\tau}}\,A_{\rm in0},$$
$$A^{\rm t}_{\rm out0} = \frac{T^2e^{i\omega_1\tau}}{1-R^2e^{2i\omega_1\tau}}\,A_{\rm in0},$$
$$A^{\rm r}_{\rm out0} = \frac{R-Re^{2i\omega_1\tau}}{1-R^2e^{2i\omega_1\tau}}\,A_{\rm in0}.$$

Amplitudes $A_{\rm in0}$, $A_{\pm0}$ and $A^{\rm r}_{\rm out0}$ are evaluated at point $x=0$ and amplitude $A^{\rm t}_{\rm out}$ at point $x=L$.

The first order solution in spectral domain is:

$$a_+ = Ta_{\rm in} - Ra_- + RA_{-0}2ik_1X_a,$$
$$a^{\rm r}_{\rm out} = Ra_{\rm in} + Ta_- + RA_{\rm in0}2ik_1X_a,$$
$$a_- = Ta_{\rm vac}e^{i(\omega_1+\Omega)\tau} - Ra_+e^{2i(\omega_1+\Omega)\tau} - RA_{+0}e^{2i\omega_1\tau}\Big[2ik_1X_b + g_+(L) - g_-(L)\Big]e^{i\Omega\tau},$$
$$a^{\rm t}_{\rm out} = Ra_{\rm vac} + Ta_+e^{i(\omega_1+\Omega)\tau}.$$

Here $a_i = a_i(\omega_1+\Omega)$, $g_\pm(x) = g_\pm(x,\omega_1+\Omega)$ and $X_i = X_i(\Omega)$. Spectral amplitudes $a_{\rm in}$, $a_\pm$ and $a^{\rm r}_{\rm out}$ are evaluated at point $x=0$ and amplitude $a^{\rm t}_{\rm out}$ at point $x=L$. The first order solution is:

$$a_+ = \frac{T}{1-R^2e^{2i(\omega_1+\Omega)\tau}}\,a_{\rm in} - \frac{RTe^{i(\omega_1+\Omega)\tau}}{1-R^2e^{2i(\omega_1+\Omega)\tau}}\,a_{\rm vac} + \frac{R^2A_{+0}e^{2i\omega_1\tau}}{1-R^2e^{2i(\omega_1+\Omega)\tau}}\,i\Big[2k_1\Big(X_be^{i\Omega\tau}-X_a\Big)+\delta\Psi_{\rm gw+emw}\Big],$$
$$a_- = -\frac{RTe^{2i(\omega_1+\Omega)\tau}}{1-R^2e^{2i(\omega_1+\Omega)\tau}}\,a_{\rm in} + \frac{Te^{i(\omega_1+\Omega)\tau}}{1-R^2e^{2i(\omega_1+\Omega)\tau}}\,a_{\rm vac} + \frac{A_{-0}}{1-R^2e^{2i(\omega_1+\Omega)\tau}}\,i\Big[2k_1\Big(X_be^{i\Omega\tau}-\rho_1X_a\Big)+\delta\Psi_{\rm gw+emw}\Big],$$
$$a^{\rm t}_{\rm out} = \frac{T^2e^{i(\omega_1+\Omega)\tau}}{1-R^2e^{2i(\omega_1+\Omega)\tau}}\,a_{\rm in} + \frac{R-Re^{2i(\omega_1+\Omega)\tau}}{1-R^2e^{2i(\omega_1+\Omega)\tau}}\,a_{\rm vac} + \frac{R^2A^{\rm t}_{\rm in0}e^{2i\omega_1\tau}}{1-R^2e^{2i(\omega_1+\Omega)\tau}}\,i\Big[2k_1\Big(X_be^{i\Omega\tau}-X_a\Big)+\delta\Psi_{\rm gw+emw}\Big]e^{i\Omega\tau},$$
$$a^{\rm r}_{\rm out} = \frac{R-Re^{2i(\omega_1+\Omega)\tau}}{1-R^2e^{2i(\omega_1+\Omega)\tau}}\,a_{\rm in} + \frac{T^2e^{i(\omega_1+\Omega)\tau}}{1-R^2e^{2i(\omega_1+\Omega)\tau}}\,a_{\rm vac} + \frac{TA_{-0}}{1-R^2e^{2i(\omega_1+\Omega)\tau}}\,i\Big[2k_1\Big(X_be^{i\Omega\tau}-\sigma_1X_a\Big)+\delta\Psi_{\rm gw+emw}\Big],$$

where $\rho_1(\Omega) = R^2e^{2i(\omega_1+\Omega)\tau}$ and $\delta\Psi_{\rm gw+emw} = 2k_1\big[g_+(L)-g_-(L)\big]e^{i\Omega\tau}$. Factor σ_1 is introduced in Sec. II.

APPENDIX D: SINE QUADRATURE

In this Appendix we calculate explicitly the DFI response signal in the case of measurement of the sine quadratures.

The Fourier image of the sine quadrature $\mathfrak{a}$ corresponding to the field amplitude $a(\omega_0+\Omega)$ is (see Appendix A):

$$\mathfrak{a}(\Omega) = \frac{a(\omega_0+\Omega) - a^\dagger(\omega_0-\Omega)}{\sqrt{2}i}.$$

We will keep the same Gothic notations for the cosine and sine quadratures in order not to introduce a huge amount of new notations. Assuming again $\mathcal{A}/\mathcal{T}^2_{\delta_1} = \mathcal{B}/\mathcal{T}^2_{\delta_2} \in \mathbb{R}$ we obtain:

$$\mathfrak{a}^{\rm r}_{\rm out} = \frac{\mathcal{R}_1a_{\rm in} - \mathcal{R}^*_{1-}a^\dagger_{\rm in-}}{\sqrt{2}i} + \frac{\mathcal{T}_1a_{\rm vac} - \mathcal{T}^*_{1-}a^\dagger_{\rm vac-}}{\sqrt{2}i} + \frac{\mathcal{A}}{\mathcal{T}^2_{\delta_1}}\sqrt{2}ik_0\Big[\mu_1(\xi_b+\xi_{\rm gw})e^{i\Omega\tau} - \nu_1\xi_a\Big],$$
$$\mathfrak{a}^{\rm t}_{\rm out} = \frac{\mathcal{T}_1a_{\rm in} - \mathcal{T}^*_{1-}a^\dagger_{\rm in-}}{\sqrt{2}i} + \frac{\mathcal{R}_1a_{\rm vac} - \mathcal{R}^*_{1-}a^\dagger_{\rm vac-}}{\sqrt{2}i} + \frac{\mathcal{A}}{\mathcal{T}^2_{\delta_1}}\sqrt{2}ik_0\Big[\eta_1(\xi_b+\xi_{\rm gw})e^{2i\Omega\tau} - \eta_1\xi_ae^{i\Omega\tau}\Big],$$
$$\mathfrak{b}^{\rm r}_{\rm out} = \frac{\mathcal{R}_2b_{\rm in} - \mathcal{R}^*_{2-}b^\dagger_{\rm in-}}{\sqrt{2}i} + \frac{\mathcal{T}_2b_{\rm vac} - \mathcal{T}^*_{2-}b^\dagger_{\rm vac-}}{\sqrt{2}i} + \frac{\mathcal{B}}{\mathcal{T}^2_{\delta_2}}\sqrt{2}ik_0\Big[\mu_2(-\xi_a+\xi_{\rm gw})e^{i\Omega\tau} + \nu_2\xi_b\Big],$$
$$\mathfrak{b}^{\rm t}_{\rm out} = \frac{\mathcal{T}_2b_{\rm in} - \mathcal{T}^*_{2-}b^\dagger_{\rm in-}}{\sqrt{2}i} + \frac{\mathcal{R}_2b_{\rm vac} - \mathcal{R}^*_{2-}b^\dagger_{\rm vac-}}{\sqrt{2}i} + \frac{\mathcal{B}}{\mathcal{T}^2_{\delta_2}}\sqrt{2}ik_0\Big[\eta_2(-\xi_a+\xi_{\rm gw})e^{2i\Omega\tau} + \eta_2\xi_be^{i\Omega\tau}\Big],$$

where

$$\mu_j(\Omega) = -\frac{RT^2}{i\mathfrak{T}_j}\,2\big(\cos2\delta_j\tau - R^2e^{2i\Omega\tau}\big),$$
$$\nu_j(\Omega) = -\frac{R}{i\mathfrak{T}_j}\Big[2\big(1+R^4e^{2i\Omega\tau}+R^4e^{4i\Omega\tau}\big) - 2R^2\cos2\delta_j\tau\big(1+2e^{2i\Omega\tau}+R^2e^{4i\Omega\tau}\big) + 2R^2e^{2i\Omega\tau}\cos4\delta_j\tau\Big],$$

$$\eta_j(\Omega) = \frac{R^2T^2}{i\mathfrak{T}_j}\,2\big(\cos 3\delta_j\tau - R^2 e^{2i\Omega\tau}\cos\delta_j\tau\big).$$

Performing the three-steps noise-cancelation algorithm we obtain the following DFI response signal:

$$\mathfrak{s} = \mathfrak{s}^{\rm fl} + \frac{\mathcal{A}}{\mathcal{T}^2_{\delta_1}}\sqrt{2}ik_0(\mu_1-\nu_1)\xi_{\rm gw}e^{2i\Omega\tau},$$

where $\mu_1-\nu_1 = -2iR(1-\cos 2\delta_1\tau)$. In narrow-band and long-wave approximations $\mu_1-\nu_1 \approx -4i(\delta_1\tau)^2$ and for the terms describing optical noise we can assume $\mu_i \approx \nu_i \approx -\eta_i$. Then the DFI response signal reduces to:

$$\begin{aligned}\mathfrak{s}|_{\delta_2=\delta_1} &= \mathfrak{s}|_{\delta_2=-\delta_1}\\ &\approx \mathfrak{a}_{\rm in} + \mathfrak{b}_{\rm in} + \mathfrak{a}_{\rm vac} + \mathfrak{b}_{\rm vac} + \delta_1\tau\,\frac{\delta_1}{\gamma - i\delta_1}\,\mathcal{A}\sqrt{2}k_0Lh,\end{aligned}$$

where $\mathfrak{a}_{\rm in} = (a_{\rm in} - a^\dagger_{\rm in-})/(\sqrt{2}i)$ and so on. Note that the quantity $\mu_1-\nu_1$ is $\delta_1\tau$ times smaller than the similar quantity $\alpha_1-\beta_1$ in the case of the cosine quadrature (see Sec. III).

[1] R. Weiss, Quarterly Progress Report, Research Lab. of Electronics, M.I.T. **105**, 54 (1972).
[2] L. Ju, D.G. Blair and C. Zhao, Rep. Prog. Phys. **63**, 1317 (2000).
[3] A. Abramovici *et al.*, Science **256**, 325 (1992).
[4] D. Sigg *et al.*, Class. Quantum Grav. **23**, S51 (2006).
[5] *LIGO website*, URL `http://www.ligo.caltech.edu`.
[6] F. Acernese *et al.*, Class. Quantum Grav. **23**, S635 (2006).
[7] *VIRGO website*, URL `http://www.virgo.infn.it`.
[8] H. Luck *et al.*, Class. Quantum Grav. **23**, S71 (2006).
[9] *GEO-600 website*, URL `http://geo600.aei.mpg.de`.
[10] M. Ando *et al.*, Class. Quantum Grav. **22**, S881 (2005).
[11] *TAMA-300 website*, URL `http://tamago.mtk.nao.ac.jp`.
[12] D.E. McClelland *et al.*, Class. Quantum Grav. **23**, S41 (2006).
[13] *ACIGA website*, URL `http://www.anu.edu.au/Physics/ACIGA`.
[14] A. Weinstein, Class. Quantum Grav. **19**, 1575 (2002).
[15] *Advanced LIGO website*, URL `http://www.ligo.caltech.edu/advLIGO/scripts/summary.shtml`.
[16] K. Kuroda, Class. Quantum Grav. **23**, S215 (2006).
[17] V.B. Braginsky and F.Ya. Khalili, *Quantum Measurement* (Cambridge University Press, Cambridge, 1992).
[18] V.B. Braginsky, Sov. Phys. JETP **26**, 831 (1968).
[19] V.B. Braginsky and Yu.I. Vorontsov, Sov. Phys. Usp. **17**, 644 (1975).
[20] V.B. Braginsky, Yu.I. Vorontsov and F.Ya. Khalili, Sov. Phys. JETP **46**, 705 (1977).
[21] H.J. Kimble *et al.*, Phys. Rev. D **65**, 022002 (2002), arXiv:gr-qc/0008026v2.
[22] F.Ya. Khalili, Phys. Lett. A **298**, 308 (2002), arXiv:gr-qc/0203002v1.
[23] S.L. Danilishin and F.Ya. Khalili, Phys. Lett. A **300**, 547 (2002), arXiv:gr-qc/0202100v4.
[24] F.Ya. Khalili, Phys. Lett. A **317**, 169 (2003), arXiv:gr-qc/0304060v1.
[25] S.L. Danilishin and F.Ya. Khalili, Phys. Rev. D **73**, 022002 (2006), arXiv:gr-qc/0508022v1.
[26] F.Ya. Khalili, Phys. Rev. D **75**, 082003 (2007).
[27] S. Kawamura and Y. Chen, Phys. Rev. Lett. **93**, 211103 (2004), arXiv:gr-qc/0405093v2.
[28] Y. Chen and S. Kawamura, Phys. Rev. Lett. **96**, 231102 (2006), arXiv:gr-qc/0504108v3.
[29] Y. Chen *et al.*, Phys. Rev. Lett **97**, 151103 (2006), arXiv:gr-qc/0603054v2.
[30] C.M. Caves, Phys. Rev. D **23**, 1693 (1981), arXiv:gr-qc/0405093v2.
[31] W.K. Unruh, *Experimental Gravitation, and Measurement Theory* (Plenum, New York, 1982), p. 647.
[32] V.B. Braginsky and F.Ya. Khalili, Rev. Mod. Phys. **68**, 1 (1996).
[33] C. Misner, K. Thorne and J. Wheeler, *Gravitation*, vol. 3 (San Francisco, W.H. Freeman and Company, 1973).
[34] R. Blandford and K.S. Thorne, *Ph 136: Applications of Classical Physics* (California Institute of Technology, Pasadena, 2003), chap. 26, URL `http://www.pma.caltech.edu/Courses/ph136/yr2002/chap26/0226.1.pdf`.
[35] E.E. Flanagan and S.A. Hughes, New J. Phys. **7**, 204 (2005), arXiv:gr-qc/0501041v3.
[36] M. Rakhmanov, Phys. Rev. D **71**, 084003 (2005), arXiv:gr-qc/0406009v1.
[37] S.P. Tarabrin, Phys. Rev. D **75**, 102002 (2007), arXiv:gr-qc/0701156v2.
[38] S.P. Tarabrin and S.P. Vyatchanin, paper in preparation.
[39] K. Somiya *et al.*, *Isolation of gravitational waves from displacement noise and utility of a time-delay device*, arXiv:gr-qc/0610117v2.
[40] K. Somiya *et al.*, Phys. Rev. Lett **76**, 022002 (2007).
[41] S.P. Vyatchanin, paper in preparation.
[42] V.B. Braginsky and A.B. Manukin, Sov. Phys. JETP **25**, 653 (1967).
[43] V.B. Braginsky, M.L. Gorodetsky and F.Ya. Khalili, Phys. Lett. A **232**, 340 (1997).
[44] V.B. Braginsky and F.Ya. Khalili, Phys. Lett. A **257**, 241 (1999).
[45] M. Rakhmanov, Ph.D. thesis, California Institute of Technology (2000), URL `http://www.ligo.caltech.edu/docs/P/P000002-00.pdf`.
[46] F.Ya. Khalili, Phys. Lett. A **288**, 251 (2001), arXiv:gr-qc/0107084.
[47] A. Buonanno and Y. Chen, Phys. Rev. D **64**, 042006 (2001), arXiv:gr-qc/0102012.
[48] A. Buonanno and Y. Chen, Phys. Rev. D **65**, 042001 (2001), arXiv:gr-qc/0107021.
[49] V.I. Lazebny and S.P. Vyatchanin, Phys. Lett. A **344**, 7 (2005).
[50] F.Ya. Khalili, V.I. Lazebny and S.P. Vyatchanin, Phys. Rev. D **73**, 062002 (2006), arXiv:gr-qc/0511008.
[51] S.P. Tarabrin and S.P. Vyatchanin, paper in preparation.
[52] M. Rakhmanov, private communication; paper in preparation.

[53] C.K. Law, Phys. Rev. A **51**, 2537 (1995).
[54] C.M. Caves and B.L. Schumaker, Phys. Rev. A **31**, 3068 (1985).
[55] B.L. Schumaker and C.M. Caves, Phys. Rev. A **31**, 3093 (1985).